

# The *Gaia* white dwarf revolution

Pier-Emmanuel Tremblay<sup>a</sup>, Antoine Bédard<sup>a</sup>, Mairi W. O’Brien<sup>a</sup>, James Munday<sup>a</sup>, Abigail K. Elms<sup>a</sup>, Nicola Pietro Gentillo Fusillo<sup>b</sup>, Snehalata Sahu<sup>a</sup>

<sup>a</sup>*Department of Physics, University of Warwick, Coventry, CV4 7AL, UK*

<sup>b</sup>*Università degli studi di Trieste, Via Valerio, 2, Trieste, 34127, Italy*

---

## Abstract

This review highlights the role of the *Gaia* space mission in transforming white dwarf research. These stellar remnants constitute 5-7% of the local stellar population in volume, yet before *Gaia* the lack of trigonometric parallaxes hindered their identification. The mission’s Data Release 2 in 2018 provided the first unbiased colour-absolute magnitude diagram of the local stellar population, identifying 260 000 white dwarfs, with the number later increasing to over 355 000 in Data Release 3. Since then, more than 400 white dwarf studies have made critical use of *Gaia* data, establishing it as a fundamental resource for white dwarf identification, fundamental parameter determination and more recently spectral type characterisation. The review underscores the routine reliance on *Gaia* parallaxes and extensive use of its photometry in white dwarf surveys. We also discuss recent discoveries firmly grounded in *Gaia* data, including white dwarf mergers, exotic compact binaries and evolved planetary systems.

*Keywords:* white dwarfs, astrometry, stars: evolution, stars: statistics, (Galaxy:) solar neighborhood

*PACS:* 0000, 1111

*2000 MSC:* 0000, 1111

---

## 1. Introduction

At the end of the life cycle of a star less massive than 8–10  $M_{\odot}$ , the remaining core, composed mostly of carbon, oxygen, and in some cases neon, contracts into a white dwarf. These are the most common stellar remnants,

accounting for 5-7% of the local stellar population in volume (Gaia Collaboration et al., 2021). White dwarfs are characterized by their Earth-like radii and correspondingly low luminosities. In the local volume, their luminosity distribution peaks within the range of  $10^{-3}$  to  $5 \times 10^{-5} L_{\odot}$ . They gradually cool over time, and their cooling track in a Hertzsprung-Russell (HR) diagram has long been used to date stellar populations.

Until *Gaia*, local stellar volume samples were limited to  $\approx 500$  white dwarfs within  $\approx 50$  pc of the Sun (Limoges et al., 2015; Holberg et al., 2016), and several thousands more at larger distances identified from Sloan Digital Sky Survey (SDSS) spectroscopy (York et al., 2000; Kepler et al., 2019). This situation arose from the challenge of distinguishing cool white dwarfs from main-sequence stars based solely on photometry, without the aid of a distance estimate. The sample of white dwarfs with trigonometric parallax measurements was itself limited to about  $\approx 200$  objects (Bergeron et al., 2001; Subasavage et al., 2017; Bédard et al., 2017; Leggett et al., 2018), with some of the most precise constraints originating from the 20 white dwarfs observed by *Hipparcos* (Vauclair et al., 1997). Decades of effort have enabled the definition and comparison of two independent methods for acquiring white dwarf parameters (effective temperature –  $T_{\text{eff}}$ , mass, radius, luminosity, surface gravity –  $\log g$ , surface chemical composition and cooling age): the photometric and astrometric technique (Koester et al., 1979; Bergeron et al., 2001); and the spectroscopic method (Bergeron et al., 1992). The large independence of these two approaches is anchored in the well-constrained white dwarf mass-radius relation (Parsons et al., 2017; Tremblay et al., 2017; Bédard et al., 2017).

Since the launch of *Gaia* in 2013, the mission has been collecting a comprehensive all-sky sample of astrometric data (position, parallax, proper motion) and apparent magnitudes in three broad optical filters ( $G$ ,  $G_{\text{BP}}$ ,  $G_{\text{RP}}$ ; Gaia Collaboration et al. 2016). Its Data Release 1 (DR1) sample included only six directly observed white dwarfs but several more in wide binaries for which the companion had a parallax (Tremblay et al., 2017). The situation changed dramatically on 25 April 2018, when *Gaia* DR2 was able to draw for the first time the HR diagram of the local stellar population including over 260 000 white dwarfs (Gaia Collaboration et al., 2018; Jiménez-Esteban et al., 2018; Gentile Fusillo et al., 2019). This number later increased to over

355 000 white dwarfs in *Gaia* EDR3/DR3<sup>1</sup>. Since then, more than 400 white dwarf studies have used *Gaia* data<sup>2</sup> as a fundamental input. The focus of this review is to illustrate the progress made in white dwarf research thanks to *Gaia* DR2 and DR3 data through these recent studies. For further background, we refer to the bibliography of this work, as well as several reviews on white dwarf evolution, atmospheres, magnetic fields, constitutive physics and pulsations (Fontaine et al., 2001; Althaus et al., 2010; Ferrario et al., 2020; Saumon et al., 2022; Bédard, 2024), as well as their evolved planetary systems (Farihi, 2016; Veras, 2021; Xu et al., 2024).

It is now routine for white dwarf studies to rely on *Gaia* parallaxes as it is by far the largest and most precise such dataset. *Gaia* (spectro-)photometry also features prominently in recent white dwarf characterisations. This review emphasises the significance of survey papers utilising extensive *Gaia* datasets but also noteworthy are high-profile findings on rare individual white dwarfs, such as mergers (Caiazzo et al., 2023), exotic compact binaries (Burdge et al., 2022) and evolved planetary systems (Vanderburg et al., 2020), all firmly grounded in *Gaia* data. We acknowledge the significant contributions of the *Gaia* DPAC team, whose crucial work and papers have allowed the community results presented herein.

## 2. *Gaia* white dwarf samples

*Gaia* data enable the characterisation of white dwarf optical colors (e.g.,  $G_{\text{BP}} - G_{\text{RP}}$  in magnitude units), which are primarily determined by the  $T_{\text{eff}}$  and atmospheric composition. Additionally, *Gaia* photometry and parallax provide absolute magnitudes (e.g.,  $G_{\text{abs}}$ ), which depend on the  $T_{\text{eff}}$ , atmospheric composition and radius. Both colours and magnitudes also have a small dependence on  $\log g$ , interior composition and interstellar extinction. Using the  $T_{\text{eff}}$ -dependent white dwarf mass-radius relation, the position of a white dwarf in the *Gaia* HR diagram can be translated into a mass and luminosity. White dwarfs are characterised by faint absolute magnitudes for a given colour, hence are found in a region of the HR diagram that is pre-

---

<sup>1</sup>DR3 largely contributed to adding auxiliary data, such as low-resolution spectrophotometry, to white dwarfs already identified in EDR3. We refer to this as the DR3 white dwarf sample.

<sup>2</sup>Refereed papers from 2018 onward including both “*Gaia*” and “white dwarfs” in their abstract according to SAO/NASA Astrophysics Data System.

dicted to be otherwise empty, at least in principle for sufficiently high data quality (Fig. 1). We remind the reader that white dwarfs with larger masses have smaller radii, so those with increasingly high masses are located in the bottom left corner of the HR diagram.

Starting with *Gaia* DR2, different teams including *Gaia* DPAC have extracted *Gaia* white dwarf samples (Gaia Collaboration et al., 2018; Jiménez-Esteban et al., 2018; Gentile Fusillo et al., 2019; Pelisoli and Vos, 2019), culminating in the current DR3 samples (Gaia Collaboration et al., 2021; Gentile Fusillo et al., 2021b; Jiménez-Esteban et al., 2023). In this section we highlight the most recent white dwarf samples, as the selection process was qualitatively the same for DR2 and DR3.

Despite the apparently isolated white dwarf locus in the HR diagram, several difficulties arose in the selection of white dwarf samples for two primary reasons: statistical and systematic *Gaia* data uncertainties, as well as binary stars. Fig. 1 confirms that a simple astrometric precision cut of `PARALLAX_OVER_ERROR`  $> 1$  is not sufficient to differentiate between white dwarfs and main sequence stars. However, the intrinsic faintness of white dwarfs can actually offer an advantage in selecting them from *Gaia*, as absolute magnitudes of  $M_G \approx 12$  and 13.5 mag, which are the median for magnitude and volume-limited samples, respectively, imply parallaxes of 2.5–5 mas at  $G = 20$  mag. This is higher than the *Gaia* average parallax precision of  $\approx 0.5$  mas at the limiting magnitude of  $G \approx 20$  mag (Gaia Collaboration et al., 2023b), hence a cutoff in parallax significance (`PARALLAX_OVER_ERROR`) has been used as a compromise to retain a majority of *Gaia* white dwarfs while eliminating most other sources. Additionally, it has been shown that white dwarf candidates can also be selected through *Gaia* precise reduced proper-motion method, even if parallax significance is below  $1\sigma$  (Gentile Fusillo et al., 2021b).

Systematic issues in *Gaia* data have also impacted white dwarf selection, namely blue color excesses (through the parameter `PHOT_BP_RP_EXCESS_FACTOR`) especially in crowded regions like the Galactic plane and the Magellanic Clouds, resulting in red objects such as nearby M dwarfs and brown dwarfs contaminating the white dwarf sample. There are also issues with spurious large parallax values and high astrometric noise (through parameters `ASTROMETRIC_SIGMA5D_MAX`, `ASTROMETRIC_EXCESS_NOISE` or `RUWE`). Different methods have been proposed, both by the *Gaia* DPAC team and white dwarf community, to filter these non-white dwarf sources (see e.g. Gentile Fusillo et al. 2021b).

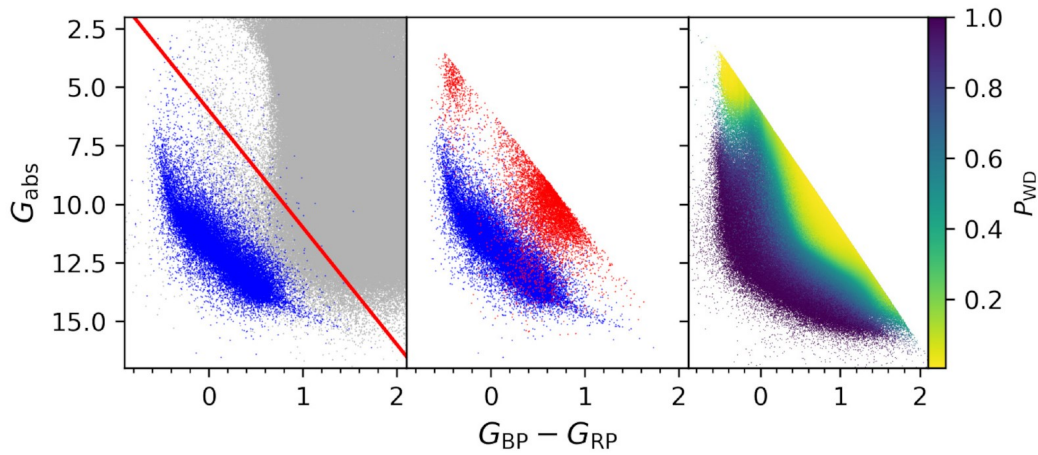


Figure 1: Example of *Gaia* EDR3 white dwarf selection from Gentile Fusillo et al. (2021b). *Left*: HR diagram showing a representative sample of 2 million random sources with a parallax precision better than 100% (gray points). The blue points represent spectroscopically confirmed white dwarfs from SDSS defining the white dwarf locus. A broad cut (red line) is used to limit the number of contaminants. *Center*: Distribution of SDSS white dwarfs (blue) and contaminants (red) included in the final selected region of the HR diagram. *Right*: Catalogue of 1280266 white dwarf candidates, with the colour scale illustrating the probability of being a white dwarf ( $P_{WD}$ ) (Source: Gentile Fusillo et al. 2021b).

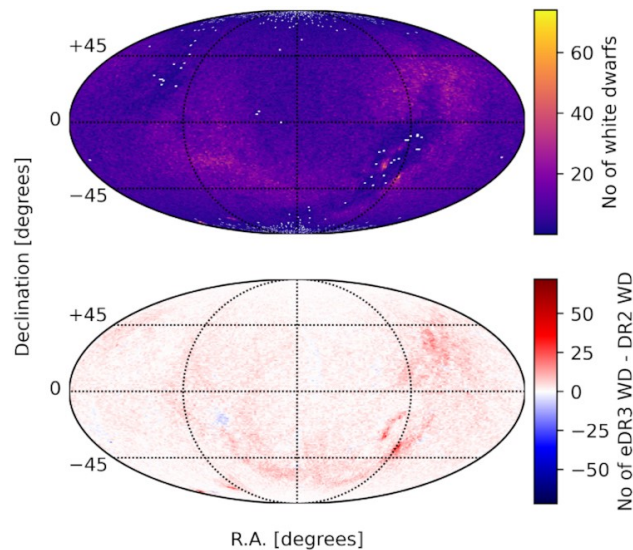


Figure 2: *Top*: Sky density (in  $1 \text{ deg}^2$  bins) of high probability *Gaia* EDR3 white dwarf candidates ( $P_{WD} > 0.75$ ). *Bottom*: Difference between EDR3 and DR2 (Source: Gentile Fusillo et al. 2021b).

By attempting to select a maximum number of *Gaia* white dwarfs, it is inevitable that they will overlap with other sources in the HR diagram. Hence, different approaches have been used to define probabilities of a source being a white dwarf, either through a direct comparison of its uncertainty contour in HR diagram compared to the locus of known white dwarfs (Gentile Fusillo et al., 2019, 2021b, see Fig. 1), or through machine learning (Gaia Collaboration et al., 2021). We note that while these *Gaia* white dwarf catalogues allow the definition of large white dwarf samples with a small contamination level, spectroscopy is needed to confirm the nature of individual white dwarf candidates.

White dwarf selection in the HR diagram is also complicated by unresolved binaries covering the full space between the white dwarf locus and the main sequence. Considerable effort has been invested in identifying binary systems including a bright, extremely low-mass white dwarf candidate (Pelisoli and Vos, 2019; Pelisoli et al., 2019), as well as unresolved white dwarf + main-sequence (hereafter WD+MS) binaries (Pala et al., 2020; Rebassa-Mansergas et al., 2021b). Compared to single white dwarfs, these systems are pushed towards the main-sequence branch of the *Gaia* HR diagram and have a lower space density, resulting in the fraction of contaminants being much larger, and the need for more stringent quality or volume cuts. Hot white dwarfs ( $T_{\text{eff}} > 30\,000$  K) are also very close to the hot subdwarfs in the HR diagram (Culpan et al., 2022), resulting in a partial overlap of these candidates even at relatively high parallax precision.

Community work has allowed the identification of  $\approx 359\,000$  high probability *Gaia* white dwarf candidates over all sky (Fig. 2). It is estimated that this represents 67–93% of all white dwarfs with  $G < 20$  mag (Gentile Fusillo et al., 2021b). Completeness is worse for hot, distant white dwarfs and better for cool, nearby sources. In particular, it is estimated that *Gaia* white dwarf completeness within 40 pc is  $>97\%$  (Hollands et al., 2018; O’Brien et al., 2024).

### 2.1. Volume-limited samples

The high *Gaia* source completeness enables the creation of representative white dwarf samples through the use of selection functions sampling the full cooling track in the HR diagram (Rix et al., 2021). However, local volume-complete samples centred around 20–100 pc of the Sun offer several advantages: they are based on decades of archival spectroscopic and photometric observations; have a much higher rate of confirmed versus candidate

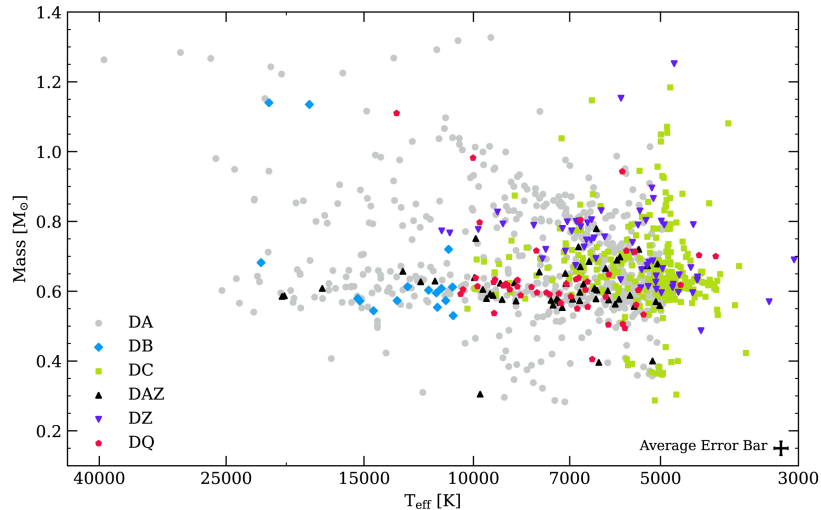


Figure 3: Model-atmosphere derived mass and  $T_{\text{eff}}$  for all 40 pc white dwarfs in DR3 as determined from *Gaia* photometry and astrometry. A correction to the parameters is implemented below 6000 K to account for model atmosphere systematics. The spectral types are indicated by the shape and colour of points, with “D” for degenerate, “A” for hydrogen Balmer lines, “B” for helium lines, “C” for no lines, “Z” for metals except carbon, and “Q” for carbon. More complex spectral types are simplified to their most prominent features. The average statistical error is shown on the lower right of the panel (Source: O’Brien et al. 2024).

white dwarfs; and are the only volumes where faint and old white dwarfs (cooling age  $\gtrsim 6$  Gyr) can be observed. The white dwarf with the faintest known luminosity, WD J2147–4035, which has one of the most evolved planetary systems around a white dwarf known to date (Elms et al., 2022), has an absolute magnitude of  $M_G = 17.73$  mag and a distance of 27.9 pc - implying it would not be detected by *Gaia* at distances larger than  $\approx 40$  pc (apparent  $G > 20.7$  mag). Local volumes of white dwarfs are essential for studies of stellar evolution, old planetary systems and Galactic star formation history.

The nearly complete 40 pc volume of spectroscopically confirmed white dwarfs was recently defined thanks to both pre-*Gaia* work (e.g. Giammichele et al. 2012; Limoges et al. 2015) and dedicated follow-up observations (Hollands et al. 2018; Tremblay et al. 2020; McCleery et al. 2020; O’Brien et al. 2023). The *Gaia* DR3 defined 40 pc sample of O’Brien et al. (2024) contains 1076 spectroscopically confirmed white dwarfs out of 1081 candidates from Gentile Fusillo et al. (2021b), hence has a completeness of 99 per cent in

white dwarf spectral types at medium-resolution (Fig. 3). However, there is a minimum of  $\approx 40$  additional white dwarfs that are found within this volume but are not identified as white dwarf candidates by Gentile Fusillo et al. (2021b), the majority of which are in unresolved WD+MS binaries (O’Brien et al., 2024; Golovin et al., 2024).

Larger volume samples are being populated by multi-object medium-resolution spectroscopic surveys (Kollmeier et al., 2017; de Jong et al., 2019; Cooper et al., 2022; Jin et al., 2024) and *Gaia* DR3 low-resolution spectrophotometry, hence more white dwarf candidates are now being confirmed. In particular, the *Gaia*-SDSS-I/IV footprint within 100 pc is nearly complete for  $T_{\text{eff}} > 7000$  K (Kilic et al., 2020b).

### 3. White dwarfs in the HR diagram

Predictions of white dwarf cooling tracks in the HR diagram (van Horn, 1968; Fontaine et al., 2001; Althaus et al., 2010; Bédard et al., 2020) have played a pivotal role in establishing connections between white dwarf populations and their Galactic environment. Before the advent of *Gaia*, determining the position of white dwarfs on the HR diagram relied on indirect methods involving model-dependent distance estimates, except for observations of globular clusters which contained a sufficient amount of white dwarfs that are all located at essentially the same distance. As such, *Gaia* DR2 (Gaia Collaboration et al., 2018) introduced the inaugural HR diagram for field white dwarfs, revealing substantial differences from the globular cluster population (refer to Fig. 4). Most notably, the *Gaia* HR diagram revealed the mysterious Q- and B-branches, at first unexplained, and not previously seen in the globular cluster populations (Richer et al., 2013).

The fundamental differences between white dwarfs observed in globular clusters and *Gaia* HR diagrams are age distributions and completeness. In globular clusters, most white dwarfs visible on the cooling sequence have formed from long-lived Sun-like stars and have a mass of  $\approx 0.53 M_{\odot}$ . White dwarfs formed from more massive and shorter-lived main-sequence stars all have large cooling ages, and are too faint to be seen or are only seen at the very bottom of the HR diagram (Richer et al., 2013). In contrast, the *Gaia* HR diagram contains stars formed at a nearly constant rate over the last  $\approx 10$  Gyr, resulting in white dwarfs of all possible ages and masses populating the diagram. We now review in turn the properties of the *Gaia* Q- and B-branches.



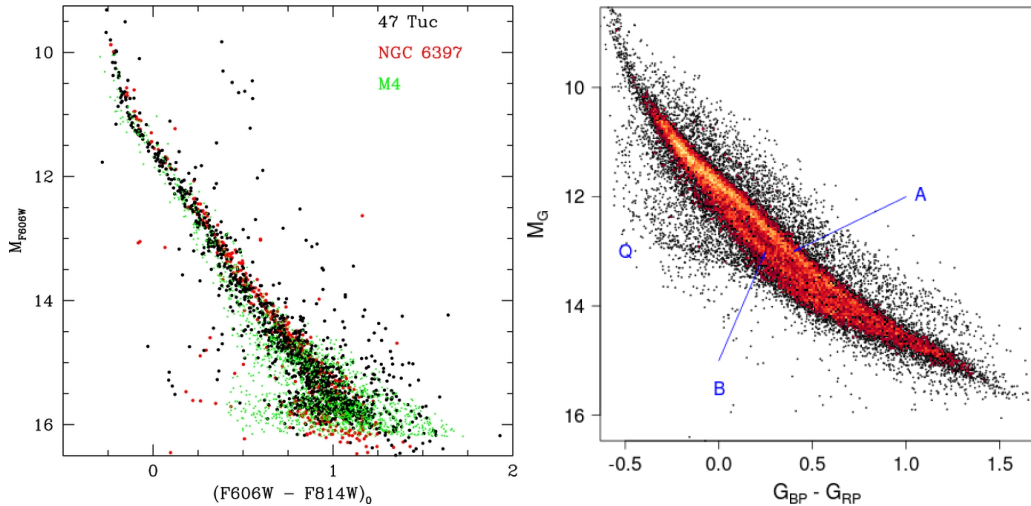


Figure 4: *Left*: Overlay of the white dwarf cooling in the globular clusters 47 Tuc, NGC 6397, and M4, as observed by the Hubble Space Telescope (Source: Richer et al. 2013). *Right*: *Gaia* DR2 HR diagram of 26 264 white dwarfs with a parallax precision better than 5%. The A-, B- and Q-branches are discussed in the text (Source: Gaia Collaboration et al. 2018).

### 3.1. Crystallisation (*Q-Branch*)

The Q-branch illustrated in Fig. 4 has been interpreted as arising from the interior crystallisation of white dwarfs and associated physical processes (Tremblay et al., 2019b). It had long been predicted that the carbon, oxygen and neon core of a white dwarf, as it cools, attains a critical temperature leading to a phase transition from liquid to solid (van Horn, 1968). This first-order phase transition releases latent heat as well as gravitational energy due to chemical separation, resulting in a cooling delay of  $\approx 1$  Gyr (Althaus et al., 2012; Blouin et al., 2020; Bauer, 2023), potentially observable in the HR diagram as a bottleneck or overdensity of white dwarfs (van Horn, 1968). Given that core crystallisation occurs at higher temperatures for higher masses, it is anticipated to generate a branch not aligned with the cooling tracks but, instead, aligned with the observed Q-branch. However, these well-known energy sources are insufficient to explain the observed overdensity, indicating that white dwarfs experience an additional  $\sim 1$  Gyr cooling delay as they crystallise (Tremblay et al., 2019b; Bergeron et al., 2019; Blouin et al., 2020; Kilic et al., 2020b). White dwarfs in wide binaries, with both components formed at the same time, present an intriguing observational

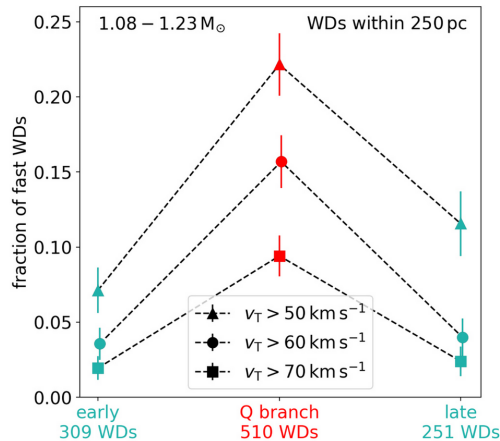


Figure 5: The fraction of fast moving white dwarfs for the mass range  $1.08\text{--}1.23 M_{\odot}$  for different tangential velocity cuts. There are significantly more fast-moving white dwarfs on the Q-branch than both above and below in the HR diagram. Fast white dwarfs are interpreted to be older than slow moving white dwarfs according to the Galactic disc age–velocity–dispersion relation. The high fraction of fast white dwarfs on the Q-branch has been interpreted as an extra cooling delay (Source: Cheng et al. 2019).

avenue for further constraining crystallisation delays if one component has started the process (Heintz et al., 2022; Venner et al., 2023).

Further insight into this problem was provided by the kinematic distribution of ultra-massive white dwarfs ( $1.08\text{--}1.23 M_{\odot}$ ) at the blue end of the Q-branch (Cheng et al., 2019, see Fig. 5). The authors demonstrated that in this mass range, *Gaia* data do not support a short cooling delay for all white dwarfs, but instead a prolonged cooling delay of  $\gtrsim 8$  Gyr for 5–9% of white dwarfs. This discovery has given rise to a substantial theoretical literature attempting to identify the nature of the powerful energy source that essentially halts the cooling (Bauer et al., 2020; Caplan et al., 2020; Horowitz, 2020; Blouin et al., 2021; Blouin and Daligault, 2021; Caplan et al., 2021; Camisassa et al., 2021). In most cases, the extra-delayed objects have been interpreted as merger products with a distinct internal chemical composition allowing for the prolonged delay, particularly a carbon/oxygen-dominated core with a high fraction of neutron-rich impurities such as  $^{22}\text{Ne}$ . The most promising solution involves enrichment in  $^{22}\text{Ne}$  and  $^{26}\text{Mg}$  by mergers of white dwarfs and subgiant stars (Shen et al., 2023), and the subsequent distillation of these elements during the crystallisation process (Blouin et al., 2021). In essence, the crystals are predicted to be depleted in neutron-rich species and

thus lighter than the surrounding liquid, implying that they float up and melt while heavier liquid is gradually displaced downward, thereby releasing a large amount of gravitational energy. White dwarf evolution models including this distillation mechanism indeed predict that the cooling is halted for  $\sim 10$  Gyr and hence successfully explain the extra-delayed population of ultra-massive white dwarfs (Bédard et al., 2024). Besides, we note that a variant of the distillation scenario for standard core compositions could also potentially explain the shorter cooling delay experienced by lower-mass white dwarfs originating from either mergers or single star evolution (Blouin et al., 2021).

### 3.2. Spectral evolution (*B-Branch*)

The A- and B-branches delineated in the *Gaia* HR diagram were promptly recognised as distinct trajectories representing the cooling of hydrogen-rich and helium-rich atmosphere white dwarfs within the temperature range of 7000–11 000 K (Gaia Collaboration et al., 2018; Gentile Fusillo et al., 2019). The prevalent A-branch consists in white dwarfs of DA spectral type characterised by their optical Balmer lines. The notably divergent B-branch is made of helium-rich atmosphere white dwarfs, predominantly of DC, DZ, and DQ spectral types (indicating no lines, metal lines, or carbon lines, respectively; see also Fig. 3). However, the large deviation between A- and B-branches cannot be explained by predicted cooling tracks based on pure-helium and pure-hydrogen model atmospheres.

The first explanation was proposed by Bergeron et al. (2019), who demonstrated that trace hydrogen with an abundance in number of  $\text{H/He} = 10^{-5}$  in helium-rich atmospheres could account for the bifurcation. Such hydrogen contamination is too small to be observed in most currently available spectroscopic observations, although the explanation remains unsatisfactory since both warmer and cooler helium-rich atmospheres are generally inconsistent with an abundance of  $\text{H/He} = 10^{-5}$  (Bergeron et al., 2022; Elms et al., 2022; Blouin et al., 2023a).

Meanwhile, investigations on the *Gaia* population of helium-atmosphere DQ white dwarfs with trace carbon (Koester and Kepler, 2019; Coutu et al., 2019; Blouin and Dufour, 2019; Koester et al., 2020; Kawka et al., 2023)<sup>3</sup> have

---

<sup>3</sup>These studies have highlighted a class of massive and warm DQ white dwarfs, possibly linked to stellar mergers and discussed in Section 4.1, and a class of average-mass cool DQ white dwarfs discussed in this section.

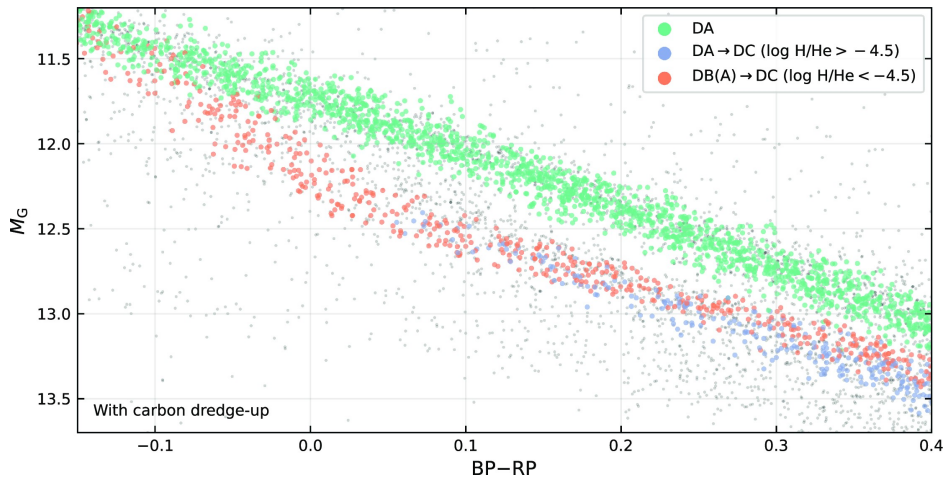


Figure 6: Gaia HR diagram of white dwarfs in the 100 pc sample (small grey dots). The coloured points show the simulation of a population of cooling pure-hydrogen (green) and helium-rich (with carbon dredge-up) white dwarf atmospheres that can explain the B-branch bifurcation. The blue and orange points for the helium-rich population distinguish objects that have and have not experienced convective mixing, respectively (Source: Blouin et al. 2023a).

led to the hypothesis that cool DQ white dwarfs may represent the upper part of the carbon pollution range resulting from convective dredge-up (Bédard et al., 2022a). In that scenario, most helium-rich DC white dwarfs may also harbour spectroscopically undetected lower traces of carbon. This scenario was recently tested through white dwarf population synthesis (Camisassa et al., 2023; Blouin et al., 2023a) and appears to provide a more plausible explanation for the B-branch bifurcation than trace hydrogen, as initially suggested by Bergeron et al. (2019). Both effects are largely degenerate for individual optical white dwarf observations, as both trace carbon and hydrogen contribute to increasing the number of free electrons and, consequently,  $\text{He}^-$  opacity. However, trace carbon offers a better fit to UV photometric observations (Blouin et al., 2023b) and to the narrowness of the B-branch in the HR diagram (Blouin et al., 2023a, see Fig. 6).

Various studies have investigated the closely related question of white dwarf spectral evolution from *Gaia* samples, examining changes in atmospheric composition during cooling. These studies largely confirmed pre-*Gaia* results, indicating that white dwarfs are born with diverse atmospheric compositions (Werner et al., 2014; Bédard et al., 2020; Reindl et al., 2023) and

then evolve into a maximum hydrogen-atmosphere DA white dwarf fraction of 90–95% within the so-called DB gap from  $\approx 40\,000$  to  $\approx 20\,000$  K (Genest-Beaulieu and Bergeron, 2019b; Ourique et al., 2019; Bédard et al., 2020; Torres et al., 2023; Vincent et al., 2024), a phenomenon attributed to element diffusion (Althaus et al., 2005; Bédard et al., 2022b, 2023). *Gaia* has also confirmed and better quantified the increase in the incidence of helium-atmosphere white dwarfs below 30 000 K (López-Sanjuan et al., 2022; Torres et al., 2023; Vincent et al., 2024; O’Brien et al., 2024). The phenomenon is most likely explained by convective dilution and mixing (Rolland et al., 2018, 2020; Cunningham et al., 2020; Bédard et al., 2022b, 2023). The fraction of helium-atmosphere white dwarfs seems to plateau at  $\approx 30\%$  for  $T_{\text{eff}} < 9000$  K, with no major spectral evolution events beyond this point (Blouin et al., 2019b; Elms et al., 2022; O’Brien et al., 2024), although this is a topic of ongoing debate (Caron et al., 2023). Spectral evolution due to the accretion of planetary debris is discussed in Section 4.3. A more extensive review of white dwarf spectral evolution is presented in Bédard (2024).

We conclude this section with the reminder that the Q- and B-branches are not observed in the HR diagram consisting of white dwarf populations in globular clusters (left panel of Fig. 4). The explanation in the former case is relatively straightforward since lower mass white dwarfs found in globular clusters have not yet solidified. The absence of the B-branch, however, remains a mystery and may suggest a not-yet understood metallicity, mass or environmental dependence in the production of helium-rich white dwarf atmospheres.

#### 4. White dwarf parameters

*Gaia* has brought about a revolution in determining white dwarf parameters. The interpretation of the *Gaia* HR diagram, as discussed in the previous section, did rely on white dwarf atmosphere and evolution models to predict colours and absolute magnitudes. In addition, several studies have explicitly derived individual *Gaia* white dwarf parameters by fitting photometry and astrometry, typically utilising synthetic fluxes from model atmospheres and the mass-radius relation specific to white dwarfs (see e.g. Gentile Fusillo et al. 2021b). In principle, this framework could enable the derivation of all fundamental white dwarf parameters solely from *Gaia* data. However, practical challenges arise due to the necessity of defining atmospheric chemical composition and interstellar extinction. Currently, these input parameters

are largely constrained by external spectroscopy and extinction maps, respectively.

Recent studies have derived the spectral types of over 100 000 white dwarfs from *Gaia* DR3 spectrophotometry (Gaia Collaboration et al., 2023a; Jiménez-Esteban et al., 2023; García-Zamora et al., 2023; Torres et al., 2023; Vincent et al., 2024), paving the way for more self-consistent parameter determinations using *Gaia* data alone. Nevertheless, for a significant portion of white dwarfs exhibiting weak lines, magnetic fields, or carbon and metal pollution, accurate parameter determinations will continue to require external medium- or high-resolution spectroscopic data (Blouin et al. 2019a; Coutu et al. 2019; Koester and Kepler 2019; Hardy et al. 2023a; Caron et al. 2023; O’Brien et al. 2024).

The *Gaia* dataset encompasses the largest number of white dwarfs, spanning all conceivable spectral types, and is distinctive for possessing the only substantial sample of parallaxes. Consequently, *Gaia* data serve as a benchmark for testing white dwarf parameter determinations employing different methods, as discussed herein. Many of these studies have relied on well-behaved hydrogen- and helium-line white dwarfs to facilitate comparisons.

***Gaia* versus optical photometry:** Comparisons with ground-based and narrower band SDSS, Pan-STARRS, J-PLUS and SkyMapper photometry have been extensively performed (Gentile Fusillo et al., 2019; Bergeron et al., 2019; López-Sanjuan et al., 2019; McCleery et al., 2020; López-Sanjuan et al., 2022; Izquierdo et al., 2023; Sahu et al., 2023). Most of these comparisons rely on the same *Gaia* astrometric data and mass-radius relation, leaving  $T_{\text{eff}}$  as the sole independent parameter. In most studies, a good agreement at the 1–2 percent level in  $T_{\text{eff}}$  has been observed for cool white dwarfs in the range 6000–10 000 K (see e.g. figure 3 of McCleery et al., 2020, for Pan-STARRS). We note that optical colours become less sensitive to  $T_{\text{eff}}$  as the latter increases, with the scatter between *Gaia* and Pan-STARRS reaching a minimum of 10% at  $T_{\text{eff}} \approx 40\,000$  K (Gentile Fusillo et al., 2019). For cool white dwarfs of all spectral types below  $\approx 6000$  K, *Gaia* astrometry has led to the identification of a significant low-mass problem, with photometric masses of white dwarfs at  $\approx 4000$  K being too small by 20% compared to predictions from Galactic population models (Hollands et al., 2018; Blouin et al., 2019b; Bergeron et al., 2019; McCleery et al., 2020; Caron et al., 2023; Cukanovaite et al., 2023; O’Brien et al., 2024; Cunningham et al., 2024). Inaccuracies of microscopic opacities in these dense, cool white dwarf atmospheres have been identified as a likely culprit (Saumon et al., 2022; Caron et al., 2023;

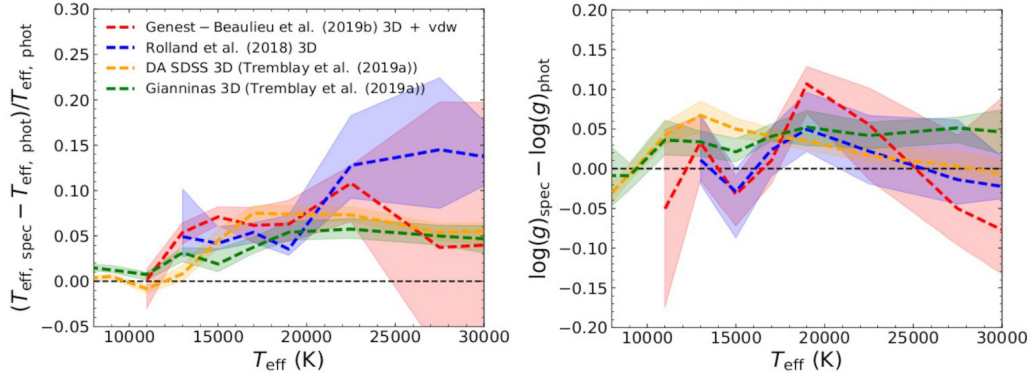


Figure 7: A comparison between *Gaia* DR3 derived  $T_{\text{eff}}$  and  $\log g$  values and spectroscopically derived parameters from the literature. The DB(A) spectroscopic parameters are from Genest-Beaulieu and Bergeron (2019b); Rolland et al. (2018) with 3D convection corrections (Cukanovaite et al., 2021). The DA spectroscopic parameters are from Gianninas et al. (2011); Tremblay et al. (2019a) with 3D convection corrections (Tremblay et al., 2013). The dashed lines indicate the median offset and the coloured areas represent the error on the median (Source: Gentile Fusillo et al. 2020).

O’Brien et al., 2024).

***Gaia* versus optical spectroscopy (line fitting):** Extensive work has been performed to compare *Gaia* photometric parameters to independent spectroscopic fits of hydrogen Balmer or helium lines (Tremblay et al., 2019a; Genest-Beaulieu and Bergeron, 2019a; Narayan et al., 2019; Gentile Fusillo et al., 2020; Tremblay et al., 2020; Gentile Fusillo et al., 2021b; Cukanovaite et al., 2021; O’Brien et al., 2023; Izquierdo et al., 2023; Axelrod et al., 2023). These studies have consistently revealed a systematic offset between the spectroscopic and photometric determinations of  $T_{\text{eff}}$  and  $\log g$  for both DA and DB(A) white dwarfs. The spectroscopic solutions yield temperatures that are 2-5% higher and surface gravities that are 0.02-0.05 dex greater (refer to Fig. 7). It has been suggested that inaccuracies in the physics of line broadening could be a contributing factor to the observed offset since most spectroscopic predictions are based on the same broadening theories. However, Fig. 7 shows that the offset is similar for DA and DB white dwarfs, exhibiting entirely different microphysics and atomic lines in their spectra. If the similarity in the offset between these two types of white dwarfs is not coincidental, this could indicate that the issue lies in the calibration of photometric measurements.

***Gaia* versus other wavelengths:** Medium-resolution far-UV spec-

trophy conducted with the Cosmic Origins Spectrograph (COS) aboard the Hubble Space Telescope (*HST*) has also been compared to *Gaia* parameters (Sahu et al., 2023). Intriguingly, the findings indicate that COS temperatures are lower than both optical spectroscopic temperatures (by 3%) and *Gaia* temperatures (by 1.5%). The analysis of mass distributions further reveals that COS masses are smaller by approximately 0.05 and 0.02  $M_{\odot}$  compared to Balmer lines and photometric masses, respectively. Recent studies have also shown the potential of DA white dwarfs as infrared flux calibrators (Gentile Fusillo et al., 2020).

**Hybrid photometric and spectroscopic methods:** Studies have added systematic errors, based on the offsets noted above, to simultaneously fit photometry, astrometry and spectroscopy (see e.g. Hollands et al., 2024). The *HST* CALSPEC flux scale (Bohlin et al. 2014; Maíz Apellániz and Weiler 2018; Bohlin et al. 2019) has also been used as part of a recipe to re-calibrate photometry for self-consistent hybrid fits, therefore enhancing the precision of white dwarf parameters (Narayan et al., 2019; Gentile Fusillo et al., 2020; Axelrod et al., 2023).

**Other methods:** The comparison between spectroscopic gravitational redshifts and *Gaia* masses and radii has been explored in recent research (Arseneau et al., 2024). An innovative white dwarf mass measurement technique for *Gaia* has been introduced by Hwang et al. (2024), demonstrating the feasibility of determining dynamical masses through wide binaries. Moreover, *Gaia* has facilitated the creation of new white dwarf catalogues, enabling the search for pulsating white dwarfs in time-domain surveys (Vincent et al., 2020; Guidry et al., 2021; Romero et al., 2022; Steen et al., 2024). This, in turn, has led to improved determinations of asteroseismic masses and temperatures, offering valuable comparisons with *Gaia* parameters (Romero et al., 2022).

#### 4.1. White dwarfs in binaries

**Resolved (wide) binaries:** The precise astrometry from *Gaia* has significantly expanded the scope of samples for wide binaries. El-Badry et al. (2021a) have compiled a catalogue featuring  $\approx 1400$  WD+WD and  $\approx 16\,000$  WD+MS wide binaries, which has been important in comparative analyses with binary population synthesis models. This revealed a notable deficit of WD+WD binaries in comparison to predictions (see also Toonen et al., 2017; O’Brien et al., 2024). El-Badry et al. (2018) found a break in the separation



distribution at 3000 au and 1500 au for WD+MS and WD+WD pairs, respectively, in significant contrast with the flatter MS+MS distribution. The authors attributed this result to white dwarfs experiencing a kick of approximately  $0.75 \text{ km s}^{-1}$  during post-main-sequence, possibly from asymmetric mass-loss. Torres et al. (2022) have conducted population synthesis fitting of the resolved binary sample within 100 pc in order to constrain the binary fraction, initial mass ratio distribution and initial separation distribution. They find the effect of the white dwarf recoil to be weaker than previously proposed by El-Badry et al. (2018). In addition, they derive a non-flat initial mass ratio distribution of  $n(q) \propto q^{-1}$ , where  $q$  is the mass ratio between the less and more massive components and thus restricted to the range [0,1]. Recent studies have also delved into the dynamic evolution of white dwarfs in triple systems (Shariat et al., 2023).

The cooling age and mass differences between individual components in wide WD+WD pairs has emerged as a promising metric for testing white dwarf evolution models (Heintz et al., 2022; Hollands et al., 2024; Heintz et al., 2024). There is a significant challenge resulting from the steep relation between main-sequence mass and lifetime, which means that canonical  $\approx 0.6 M_{\odot}$  white dwarfs with long-lived main-sequence progenitors have poorly constrained individual total ages. Hence, white dwarfs with masses  $\gtrsim 0.63 M_{\odot}$  have been favoured for model age calibration (Heintz et al., 2022).

**Unresolved double degenerates:** *Gaia* has allowed the identification of unresolved double degenerates, primarily focusing on overluminous sources above the white dwarf cooling sequence in the HR diagram. This heightened luminosity arises either from the combined flux of two white dwarfs with similar effective temperatures and masses, or from the primary white dwarf that has lost mass through mass transfer, resulting in an enlarged radius according to the mass-radius relation. Several new candidates for extremely low-mass white dwarfs have been identified prompting subsequent spectroscopic follow-up studies (Pelisoli and Vos 2019; Kawka et al. 2020; Brown et al. 2022; Kosakowski et al. 2023). Double degenerate candidates have also been identified from discrepancies between *Gaia* and spectroscopic mass estimates (see e.g. Tremblay et al., 2019a; Sahu et al., 2023).

The time-domain and spectroscopic follow-up of overluminous sources in the *Gaia* HR diagram has led to the discovery and characterisation of several short-period, double-lined compact white dwarf systems (Brown et al., 2020; Kilic et al., 2020a, 2021a,b; Kosakowski et al., 2023), some of which are eclipsing (Keller et al., 2022; Munday et al., 2023). These binary systems play a

crucial role in testing common-envelope efficiencies (Toonen et al., 2012) and predicting the gravitational wave background for space-based gravitational wave detectors such as LISA (Amaro-Seoane et al., 2017, 2023), demonstrating a clear multi-messenger harmony between *Gaia* and the gravitational wave mHz frequency regime (Lamberts et al., 2019; Korol et al., 2022; Kupfer et al., 2024; Ren et al., 2023). In particular, Korol et al. (2022) find a gap at  $\approx 1$  au in the double white dwarf separation distribution derived from *Gaia* stellar centroid astrometric wobbling (converted from RUWE parameter), which they attribute to the effect of common-envelope evolution.

**Unresolved WD+MS binaries:** Rebassa-Mansergas et al. (2021b) have identified 112 WD+MS candidates within 100 pc based on their placement in the *Gaia* DR3 HR diagram. However, they note that their selection only represents  $\approx 10\%$  of the total underlying WD+MS population, owing to *Gaia* limitations in detecting WD+MS systems with increasingly cooler white dwarfs or brighter main-sequence stars. Therefore, the exploration of such systems has necessitated additional multi-wavelength UV-*Gaia* HR diagrams (Ren et al., 2020; Anguiano et al., 2022; Nayak et al., 2023), time-domain eclipse information (Keller et al., 2022), or the detection of astrometric variations (Belokurov et al., 2020; Penoyre et al., 2022; Shahaf et al., 2023, 2024; Garbutt et al., 2024). In particular, Yamaguchi et al. (2024) have used *Gaia* DR3 astrometry to characterise a population of WD+MS candidates in relatively wide orbits (100–1000 d), which likely require a very efficient envelope ejection during common envelope evolution.

**Interacting compact binaries:** The combination of *Gaia*, follow-up spectroscopy (see e.g. Inight et al., 2023), as well as time-domain and X-ray/UV surveys has had a huge impact in identifying and characterising new interacting compact binaries. In particular, *Gaia* astrometry has allowed Pala et al. (2020, 2022) to report an updated mass distribution for 89 cataclysmic variable (CV) white dwarfs, finding a mean of  $\approx 0.8 M_{\odot}$  (compared to  $\approx 0.6 M_{\odot}$  for field white dwarfs) and no evolution of the mass with orbital period. The *Gaia* science alerts program regularly identifies outbursting CVs (Hodgkin et al., 2021). Additional work has identified a relation between period and position on the HR diagram (Abrahams et al., 2022). El-Badry et al. (2021b) presented a survey for recently detached CVs with evolved secondaries, which are proposed to be progenitors of extremely low mass white dwarfs and AM Canum Venaticorum (AM CVn) systems, characterised as hydrogen deficient compact binaries. They find that the implied Galactic birth rate of these CVs is half that of AM CVn binaries. The population

of AM CVn binaries has itself been more accurately characterised thanks to *Gaia* astrometry (Ramsay et al., 2018; Abril et al., 2020; van Roestel et al., 2022; Kupfer et al., 2024), and selection cuts reliant on *Gaia* have facilitated the discovery of new systems greatly (van Roestel et al., 2022), including the sieving of outbursting AM CVn candidates (van Roestel et al., 2021).

The varied approaches to identify and characterise compact binaries using *Gaia* data underscore the possibility of creating volume-limited samples encompassing all categories of binaries. These samples aim to be both representative of the broader population and substantial enough to act as a benchmark for future models of binary populations and gravitational wave background (Inight et al., 2021; Kawash et al., 2022; Canbay et al., 2023).

**White dwarf merger products:** The onset of white dwarf crystallisation in the *Gaia* HR diagram coincides with a distinctive statistical increase in tangential velocities (see Section 3.1). Cheng et al. (2019, 2020) used these observations to suggest that  $\approx 20\%$  of massive white dwarfs ( $0.8\text{-}1.3 M_{\odot}$ ) originate from WD+WD mergers, aligning with the predictions from Temmink et al. (2020). However, recent investigations propose that a portion of these white dwarfs may originate from mergers involving a white dwarf and a subgiant star (Shen et al., 2023). While this particular subset of merger products is predicted to experience an extra crystallisation delay (see Section 3.1), the majority of merger products (including WD+WD, WD+MS, MS+MS) are likely to display age and mass distributions close to those of white dwarfs formed from single star evolution (Temmink et al., 2020; Kilic et al., 2020b).

Efforts have been made to better characterise the subset of mergers identified by Cheng et al. (2019) through observational follow-up of massive white dwarfs. There is emerging evidence that surface carbon pollution in massive white dwarfs (hot DQ, warm DQ, DAQ spectral types; Coutu et al., 2019; Koester and Kepler, 2019; Hollands et al., 2020; Kawka et al., 2023; Kilic et al., 2024) can be explained by convective dredge-up only if the total helium and hydrogen masses are very low (Althaus et al., 2009; Hollands et al., 2020; Koester et al., 2020), which indicates a merger origin. Other indicators of mergers include large magnetic fields and rapid rotation (Kilic et al., 2023), although tracing back the evolutionary history of single massive white dwarfs remains challenging.

**Partial thermonuclear explosions:** *Gaia* has played a significant role in characterising remnants arising from incomplete or failed supernova explosions. These remnants emerge when a system, rather than undergoing a complete supernova event, undergoes partial disruption, resulting in the

formation of a white dwarf with an exotic O/Ne-dominated surface composition. Additionally, this process may propel both the white dwarf and companion star into a hyper-velocity trajectory that make them unbound from the Galaxy (Shen et al., 2018; Raddi et al., 2019; El-Badry et al., 2023; Igoshev et al., 2023; Werner et al., 2024).

We refer the reader to El-Badry (2024) for a more extensive review of stellar multiplicity in *Gaia* including compact objects.

#### 4.2. Magnetic white dwarfs

*Gaia* has played a transformative role in deriving the parameters of magnetic white dwarfs, constituting approximately 20% of the local population (Landstreet and Bagnulo, 2019). This sub-class was historically challenging to study, primarily due to the lack of both parallaxes and a quantum theory framework for combined Stark and Zeeman line broadening. Recent hybrid photometric and spectroscopic studies, relying on *Gaia* parallaxes, have determined robust atmospheric parameters for magnetic white dwarfs (see e.g. Hardy et al., 2023a,b). While fitting magnetic white dwarfs with *Gaia* photometry still faces challenges due to modified line and continuum opacities, the accuracy of *Gaia*-guided fits has been affirmed through UV and IR multi-wavelength HR diagrams. These studies demonstrate that cool magnetic white dwarfs are well-represented by non-magnetic broadband photometric models (McCleery et al., 2020). Additionally, the observation that both magnetic and non-magnetic white dwarfs crystallise at the same location in the *Gaia* HR diagram suggests not just a mere coincidence but rather similarly accurate *Gaia*-derived stellar parameters for both types.

The newly derived magnetic white dwarf parameters from *Gaia* have validated several previously hypothesised trends, which are discernible in volume-limited samples. Magnetic white dwarfs tend to be more massive than their non-magnetic counterparts (McCleery et al., 2020; Ferrario et al., 2020; Bagnulo and Landstreet, 2021; Hardy et al., 2023a; O’Brien et al., 2024). Additionally, the incidence of magnetism increases with cooling age for white dwarfs less massive than  $0.8 M_{\odot}$  (Bagnulo and Landstreet, 2022; O’Brien et al., 2024, see Fig. 8). These behaviours are not fully explained due to the origin of magnetic fields in white dwarfs still being elusive. Possible origins include stellar mergers (García-Berro et al., 2012), fossil fields (see e.g. Braithwaite and Spruit, 2004), crystallisation dynamos (see e.g. Isern et al., 2017; Ginzburg et al., 2022; Montgomery and Dunlap, 2024; Fuentes et al., 2024), main-sequence and giant-phase internal dynamos with possible

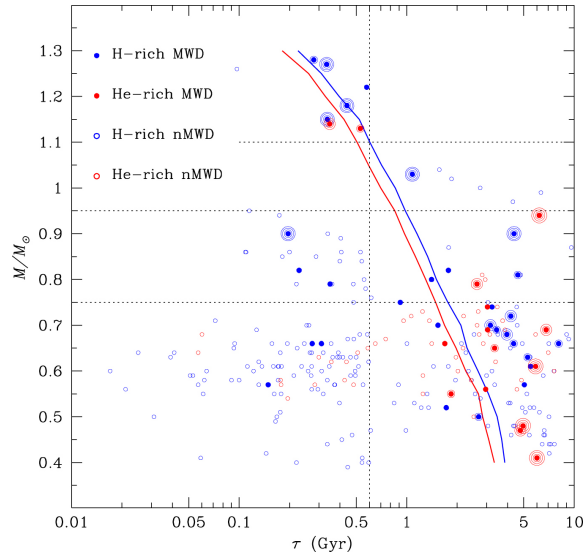


Figure 8: Cooling age-white dwarf mass diagram encompassing all white dwarfs within the local 20 pc volume and most white dwarfs aged less than 0.6 Gyr up to a distance of 40 pc. Unmarked circles represent white dwarfs devoid of detected magnetic fields, while filled dots serve to denote magnetic white dwarfs, where the level of magnetic field strength is indicated by the number of surrounding circles: one for fields below 1 MG, two for fields between 1 and 10 MG, and three for fields exceeding 100 MG. Solid curves trace the onset of core crystallisation for helium-rich (red) and hydrogen-rich (blue) atmospheres (Source: Bagnulo and Landstreet 2022).

external influence (binarity and planets; see e.g. Tout et al. 2008; Kissin and Thompson 2015), all of this complicated by a potential delay in the emergence of magnetic fields to the surface (Bagnulo and Landstreet, 2022).

A novel spectral class of DA(H)e white dwarfs, which have hydrogen-dominated atmospheres and display Balmer line emission, have been identified through *Gaia* follow-ups (Gänsicke et al., 2020; Walters et al., 2021; Manser et al., 2023; Reding et al., 2023; Elms et al., 2023; Farihi et al., 2023). This class encapsulates white dwarfs that exhibit strong magnetism ( $B > 5$  MG; DAHe), which is found in the majority of cases, and those which lack an observable magnetic field (DAe). DA(H)e white dwarfs lack close brown dwarf or stellar mass companions therefore the prevailing explanation for their observational characteristics points to an intrinsic magnetic phenomenon, potentially linked to the emergence of magnetic fields and the heightened incidence of magnetic white dwarfs for cooling ages exceeding

1–3 Gyr.

#### 4.3. Evolved planetary systems

The paradigm attributing the origin of metal atmospheric pollution in white dwarfs to the external accretion of planetary debris was established two decades ago (Jura, 2003; Zuckerman et al., 2007). *Gaia* data has significantly improved the accuracy of atmospheric chemical abundance determinations for metal-polluted D(A)(B)(Q)Z white dwarfs. This has led to a better understanding of the chemical composition and evolution of planetary systems around evolved white dwarfs (Blouin et al., 2019a; Coutu et al., 2019; Swan et al., 2019; Tremblay et al., 2020; Klein et al., 2021; Izquierdo et al., 2021; Hollands et al., 2022; Johnson et al., 2022; Blouin and Xu, 2022; O’Brien et al., 2023; Swan et al., 2023; Doyle et al., 2023; Rogers et al., 2024a; Badenas-Agusti et al., 2024).

The spectroscopic follow-up of faint and cool *Gaia* white dwarf candidates has led to the first identification of atmospheric pollution by lithium and potassium (Hollands et al., 2021; Kaiser et al., 2021; Elms et al., 2022; Vennes et al., 2024). Furthermore, the higher than expected concentrations of those elements compared to other atoms has been linked to either the accretion of crust material, the signature of Big Bang nucleosynthesis, or inaccuracies in current atomic diffusion time calculations.

The availability of large *Gaia* white dwarf catalogues has prompted investigations into infrared excesses around white dwarfs resulting from debris disks (Xu et al., 2020; Rebassa-Mansergas et al., 2019; Lai et al., 2021), gas emission from these discs (Melis et al., 2020; Manser et al., 2020; Gentile Fusillo et al., 2021a), transiting debris (Guidry et al., 2021), and the frequency of metal pollution in wide binaries (O’Brien et al., 2024; Noor et al., 2024). *Gaia* has also stimulated searches for astrometric planet candidates (Andrews et al., 2019; Sanderson et al., 2022; Kervella et al., 2022; Rogers et al., 2024b), although this area of research is still in its infancy as raw astrometric data is not yet publicly available. However, it is anticipated to become a significant focus with future data releases.

## 5. Astrophysical relations

Larger and less biased samples of white dwarfs, along with more precise and accurate stellar parameters, have contributed to the improved calibration

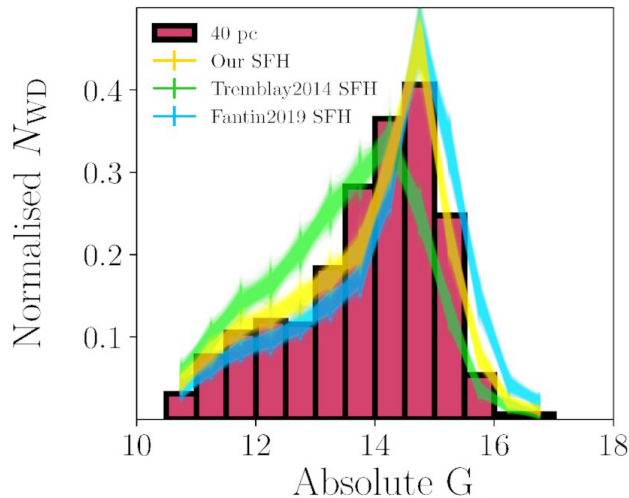


Figure 9: Normalised histogram of the absolute *Gaia*  $G$  magnitudes for the 40 pc volume-limited sample (black). The three contours show the results (and uncertainties) of population synthesis models using three different parameterisation for the star formation rate. A uniform rate for the last 10.6 Gyr is plotted in yellow. In green and blue are simulated populations relying on the stellar formation history of Tremblay et al. (2014) and Fantin et al. (2019), respectively (Source: Cukanovaite et al. 2023).

of fundamental astrophysical relations using white dwarfs. This process typically begins by modelling the kinematic distribution (Fig. 5), absolute magnitude (or luminosity) distribution (Fig. 9) and mass distribution (Fig. 10) of white dwarfs.

The initial-final mass relation (IFMR), which connects the masses of the progenitor main-sequence star and the white dwarf, is pivotal for constraining mass loss in stellar evolution and determining the total age of white dwarf populations. Leveraging the *Gaia* white dwarf mass distribution in volume-limited samples (Fig. 10), El-Badry et al. (2018) and Cunningham et al. (2024) have introduced a novel statistical method to derive the IFMR (Fig. 11). This technique ensures that the predicted total age of a white dwarf (time since zero-age main sequence) is self-consistent with white dwarf masses determined from *Gaia* data and aligns with our general understanding of Galactic disc age, star formation rate and initial mass function (IMF).

Equally important studies have employed *Gaia*-characterised wide binaries (Barrientos and Chanamé, 2021; Hollands et al., 2024) and stellar clusters (Marigo et al., 2020) to obtain more accurate IFMRs. The advantage

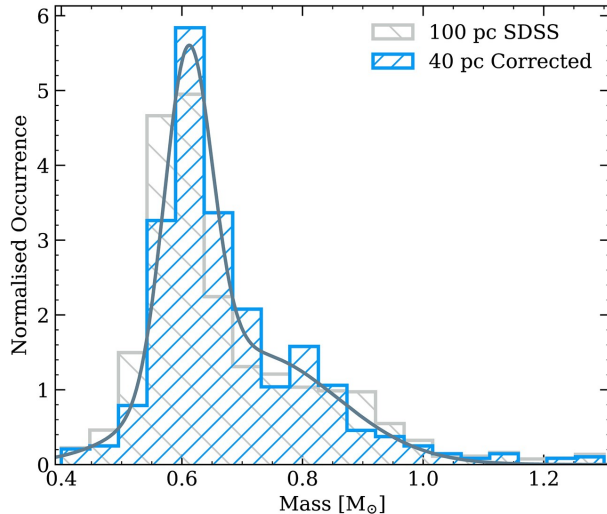


Figure 10: Mass distributions of white dwarfs in the volume complete 40 pc sample (O’Brien et al., 2024) and the 100 pc SDSS sample (Kilic et al., 2020b). The 40 pc mass distribution has been corrected for the low-mass problem at low temperatures ( $T_{\text{eff}} < 6000$  K) outlined in Section 4. The solid line represents the bimodal best-fitting Gaussians to the 40 pc mass distribution. (Source: O’Brien et al. 2024).

of these latter two techniques lies in their ability to characterise the scatter in the IFMR by incorporating external constraints on the total age of each individual white dwarf, such as the age of the cluster or wide companion. Although the (possibly intrinsic) scatter in the IFMR persists at the  $\approx 5\%$  level (Hollands et al., 2024), the median IFMR is statistically equivalent across most studies and white dwarf masses (see Fig. 11).

The *Gaia* HR diagram has been used to deduce the local star formation rate in the Galactic disc, employing both stars and white dwarfs. In the latter case, Cukanovaite et al. (2023) utilised the *Gaia* absolute magnitude distribution of 40 pc white dwarfs, demonstrating its consistency with a constant star formation rate over the last  $\approx 10.6$  Gyr (see Fig. 9). However, alternative studies have instead suggested star formation peaks at either early or late times (Fantin et al., 2019; Isern, 2019; Fleury et al., 2022). Explorations of star formation histories have also expanded to include the Galactic halo, demonstrating that white dwarfs serve as a suitable tool for inferring halo age and local space density (Kilic et al., 2019; Torres et al., 2021; Fantin et al., 2021), although halo age remains sensitive to systematic uncertainties



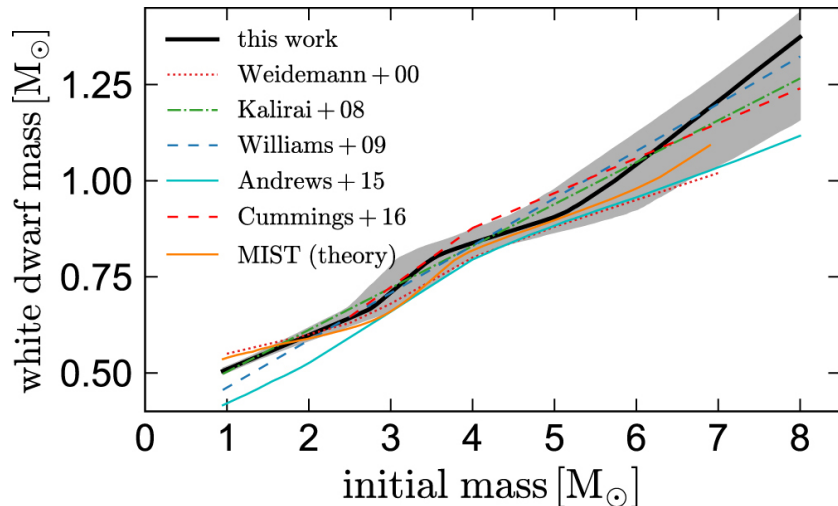


Figure 11: Best-fit population synthesis model initial-final mass relation from the *Gaia* 100 pc white dwarf sample (“this work” curve and error contour) compared to other results from the literature (Source: El-Badry et al. 2018).

in stellar evolution models. In particular, Kilic et al. (2019) and Torres et al. (2021) derive a Galactic inner halo age of  $10.9 \pm 0.4$  Gyr and  $12 \pm 0.5$  Gyr, respectively.

Coupling the local star formation history and the IFMR is the IMF. While it has historically been studied using young stellar clusters that have not yet formed white dwarfs, recent studies have constrained the IMF using the local and globular cluster populations including white dwarfs (Dickson et al., 2023; Kirkpatrick et al., 2024), finding consistency in the  $1\text{--}8 M_{\odot}$  initial-mass range with the long-established Kroupa and Salpeter IMFs.

White dwarf kinematics have been investigated using *Gaia* proper motions and external radial velocity measurements. This has been employed to derive the age versus velocity dispersion relation and Galactic radial migration history (Torres et al., 2019; Rowell and Kilic, 2019; Mikkola et al., 2022; Raddi et al., 2022; Cukanovaite et al., 2023). These relations are independent and complementary to those derived from local main-sequence stars, and are critical to extract the local star formation history (Cukanovaite et al., 2023). Due to their motions through space, the large majority of *Gaia* white dwarfs currently within 100 pc of the Sun have formed further away. Understanding the kinematic origin of the local white dwarf sample allows us to place its stellar formation history into the context of Milky Way evolution. In a

recent study, Zubiaur et al. (2024) use *Gaia* Galactic orbital parameters to find that 68% of current 100 pc white dwarfs were stars born within 1 kpc from the Sun.

Given that white dwarfs lack original metallicity information, precise radial velocities play a crucial role in making white dwarfs a tracer of Milky Way evolution (Raddi et al., 2022). Directly measured astrometric *Gaia* radial velocities is a promising avenue for extracting 3D velocities of white dwarfs with weak spectral signatures (Lindegren and Dravins, 2021). *Gaia* white dwarfs have also proven useful in age determinations of coeval and comoving young local stellar associations (Torres et al., 2019; Gagné et al., 2020).

Assuming that white dwarf ages are better, or at least as well understood as the ages of local main-sequence stars, the former have been employed to calibrate several main-sequence age relations, including isochrone fitting, age-velocity dispersion, age-activity and age-metallicity relations (Fouesneau et al., 2019; Qiu et al., 2021; Moss et al., 2022; Heintz et al., 2022; Rebassa-Mansergas et al., 2021a; Zhang et al., 2023; Rebassa-Mansergas et al., 2023). Despite these efforts, there remains a significant scatter between different methods for determining main-sequence and white dwarf ages, most prominently seen in the WD+MS and WD+WD wide binary samples (Qiu et al., 2021; Heintz et al., 2024).

In open clusters, *Gaia* has facilitated the identification of new white dwarfs and confirmation of existing members (see e.g. Griggio et al., 2022). This allowed refining age determinations of well known nearby open clusters such as the Hyades and Praesepe (Salaris and Bedin, 2018, 2019; Lodieu et al., 2019a,b), identifying new magnetic or exotic white dwarfs in clusters, suggesting that magnetic white dwarfs may form in isolation (Caiazzo et al., 2020), and providing new insights into the high-mass end of the IFMR (Prišegen et al., 2021; Richer et al., 2021; Heyl et al., 2022; Prišegen and Faltová, 2023; Griggio et al., 2022; Miller et al., 2023). *Gaia* has also been useful in improving HR diagrams of globular clusters including white dwarfs (Sahu et al., 2022).

*Gaia* white dwarf catalogues have also enhanced our understanding of local stellar extinction, particularly in determining GALEX UV reddening coefficients (Wall et al., 2019). Accurate extinction measurements are crucial for both white dwarf selection (Gentile Fusillo et al., 2021b) and obtaining accurate atmospheric parameters (Sahu et al., 2023).

Finally, *Gaia* data have played a crucial role in testing the white dwarf

mass-radius relation through the combination of spectroscopic, photometric and gravitational redshift measurements (Joyce et al., 2018; Tremblay et al., 2019a; Genest-Beaulieu and Bergeron, 2019a; Arseneau et al., 2024; Pasquini et al., 2023). The mass-radius relation has also been constrained via a combination of *Gaia* and *HST* astrometric microlensing (McGill et al., 2018, 2023). These studies have confirmed that current theoretical mass-radius relations are appropriate (Renedo et al., 2010; Romero et al., 2019; Bédard et al., 2020; Salaris et al., 2022).

## 6. Future

The number of high-probability *Gaia* white dwarf candidates has experienced a 38% increase between DR2 and DR3, and this trend is expected to continue with upcoming data releases. Despite the identification of over 355 000 white dwarf candidates in *Gaia* DR3, only approximately 10% have undergone medium-resolution spectroscopic follow-up (Gentile Fusillo et al., 2021b). As new multi-object spectroscopic surveys such as DESI, WEAVE, SDSS-V and 4MOST observe more white dwarfs in the coming decade, the scientific yield from existing *Gaia* data releases is anticipated to further increase, particularly for the rare and exotic spectral classes discussed in this review.

The combination of *Gaia* epoch photometry and astrometry in future data releases with external time-domain surveys like LSST (Fantin et al., 2020) and ZTF (Bellm et al., 2019) will enable the identification of more variable white dwarf systems. This includes compact binaries as sources of gravitational waves, giant planet companions down to one Saturn mass at orbital separations of 0.1–50 au (Kervella et al., 2022; Rogers et al., 2024b), and transiting rocky planetary debris (Guidry et al., 2021).

**Acknowledgement:** This work was supported by the European Research Council under the European Union’s Horizon 2020 research and innovation programme numbers 101002408 a Leverhulme Trust Research Grant (ID RPG-2020-366).

## References

Abrahams, E.S., Bloom, J.S., Szkody, P., Rix, H.W., Mowlavi, N., 2022. Informing the Cataclysmic Variable Sequence from Gaia Data: The Orbital-

- period-Color-Absolute-magnitude Relationship. *ApJ* 938, 46. doi:10.3847/1538-4357/ac87ab.
- Abril, J., Schmidtbreick, L., Ederoclite, A., López-Sanjuan, C., 2020. Disentangling cataclysmic variables in Gaia’s HR diagram. *MNRAS* 492, L40–L44. doi:10.1093/mnras1/slzl181, arXiv:1912.01531.
- Althaus, L.G., Córscico, A.H., Isern, J., García-Berro, E., 2010. Evolutionary and pulsational properties of white dwarf stars. *A&AR* 18, 471–566. doi:10.1007/s00159-010-0033-1, arXiv:1007.2659.
- Althaus, L.G., García-Berro, E., Córscico, A.H., Miller Bertolami, M.M., Romero, A.D., 2009. On the Formation of Hot DQ White Dwarfs. *ApJL* 693, L23–L26. doi:10.1088/0004-637X/693/1/L23, arXiv:0901.1836.
- Althaus, L.G., García-Berro, E., Isern, J., Córscico, A.H., Miller Bertolami, M.M., 2012. New phase diagrams for dense carbon-oxygen mixtures and white dwarf evolution. *A&A* 537, A33. doi:10.1051/0004-6361/201117902, arXiv:1110.5665.
- Althaus, L.G., Miller Bertolami, M.M., Córscico, A.H., García-Berro, E., Gil-Pons, P., 2005. The formation of DA white dwarfs with thin hydrogen envelopes. *A&A* 440, L1–L4. doi:10.1051/0004-6361:200500159, arXiv:astro-ph/0507415.
- Amaro-Seoane, P. et al., 2023. Astrophysics with the Laser Interferometer Space Antenna. *Living Reviews in Relativity* 26, 2. doi:10.1007/s41114-022-00041-y, arXiv:2203.06016.
- Amaro-Seoane, P. et al., 2017. Laser Interferometer Space Antenna. arXiv e-prints , arXiv:1702.00786doi:10.48550/arXiv.1702.00786, arXiv:1702.00786.
- Andrews, J.J., Breivik, K., Chatterjee, S., 2019. Weighing the Darkness: Astrometric Mass Measurement of Hidden Stellar Companions Using Gaia. *ApJ* 886, 68. doi:10.3847/1538-4357/ab441f, arXiv:1909.05606.
- Anguiano, B. et al., 2022. White Dwarf Binaries across the H-R Diagram. *AJ* 164, 126. doi:10.3847/1538-3881/ac8357, arXiv:2207.13992.

- Arseneau, S. et al., 2024. Measuring the Mass–Radius Relation of White Dwarfs Using Wide Binaries. *ApJ* 963, 17. doi:10.3847/1538-4357/ad2168.
- Axelrod, T. et al., 2023. All-sky Faint DA White Dwarf Spectrophotometric Standards for Astrophysical Observatories: The Complete Sample. *ApJ* 951, 78. doi:10.3847/1538-4357/acd333, arXiv:2305.07563.
- Badenas-Agusti, M., Vanderburg, A., Blouin, S., Dufour, P., Viaña, J., Seager, S., Wang, S.X., 2024. Detection and preliminary characterization of polluted white dwarfs from Gaia EDR3 and LAMOST. *MNRAS* 527, 4515–4544. doi:10.1093/mnras/stad3362, arXiv:2310.19790.
- Bagnulo, S., Landstreet, J.D., 2021. New insight into the magnetism of degenerate stars from the analysis of a volume-limited sample of white dwarfs. *MNRAS* 507, 5902–5951. doi:10.1093/mnras/stab2046, arXiv:2106.11109.
- Bagnulo, S., Landstreet, J.D., 2022. Multiple Channels for the Onset of Magnetism in Isolated White Dwarfs. *ApJL* 935, L12. doi:10.3847/2041-8213/ac84d3, arXiv:2208.02655.
- Barrientos, M., Chanamé, J., 2021. Improved Constraints on the Initial-to-final Mass Relation of White Dwarfs Using Wide Binaries. *ApJ* 923, 181. doi:10.3847/1538-4357/ac2f49, arXiv:2102.07790.
- Bauer, E.B., 2023. Carbon-Oxygen Phase Separation in Modules for Experiments in Stellar Astrophysics (MESA) White Dwarf Models. *ApJ* 950, 115. doi:10.3847/1538-4357/acd057, arXiv:2303.10110.
- Bauer, E.B., Schwab, J., Bildsten, L., Cheng, S., 2020. Multi-gigayear White Dwarf Cooling Delays from Clustering-enhanced Gravitational Sedimentation. *ApJ* 902, 93. doi:10.3847/1538-4357/abb5a5, arXiv:2009.04025.
- Bédard, A., 2024. The spectral evolution of white dwarfs: where do we stand? *Ap&SS* 369, 43. doi:10.1007/s10509-024-04307-5, arXiv:2405.01268.
- Bédard, A., Bergeron, P., Brassard, P., 2022a. On the Spectral Evolution of Hot White Dwarf Stars. III. The PG 1159-DO-DB-DQ Evolutionary Channel Revisited. *ApJ* 930, 8. doi:10.3847/1538-4357/ac609d, arXiv:2203.12045.

- Bédard, A., Bergeron, P., Brassard, P., 2023. On the Spectral Evolution of Hot White Dwarf Stars. IV. The Diffusion and Mixing of Residual Hydrogen in Helium-rich White Dwarfs. *ApJ* 946, 24. doi:10.3847/1538-4357/acbb62, arXiv:2302.05424.
- Bédard, A., Bergeron, P., Brassard, P., Fontaine, G., 2020. On the Spectral Evolution of Hot White Dwarf Stars. I. A Detailed Model Atmosphere Analysis of Hot White Dwarfs from SDSS DR12. *ApJ* 901, 93. doi:10.3847/1538-4357/abafbe, arXiv:2008.07469.
- Bédard, A., Bergeron, P., Fontaine, G., 2017. Measurements of Physical Parameters of White Dwarfs: A Test of the Mass-Radius Relation. *ApJ* 848, 11. doi:10.3847/1538-4357/aa8bb6, arXiv:1709.02324.
- Bédard, A., Blouin, S., Cheng, S., 2024. Buoyant crystals halt the cooling of white dwarf stars. *Nature* 627, 286–288. doi:10.1038/s41586-024-07102-y.
- Bédard, A., Brassard, P., Bergeron, P., Blouin, S., 2022b. On the Spectral Evolution of Hot White Dwarf Stars. II. Time-dependent Simulations of Element Transport in Evolving White Dwarfs with STELUM. *ApJ* 927, 128. doi:10.3847/1538-4357/ac4497, arXiv:2112.09989.
- Bellm, E. C. et al., 2019. The Zwicky Transient Facility: System Overview, Performance, and First Results. *PASP* 131, 018002. doi:10.1088/1538-3873/aaecbe, arXiv:1902.01932.
- Belokurov, V. et al., 2020. Unresolved stellar companions with Gaia DR2 astrometry. *MNRAS* 496, 1922–1940. doi:10.1093/mnras/staa1522, arXiv:2003.05467.
- Bergeron, P., Dufour, P., Fontaine, G., Coutu, S., Blouin, S., Genest-Beaulieu, C., Bédard, A., Rolland, B., 2019. On the Measurement of Fundamental Parameters of White Dwarfs in the Gaia Era. *ApJ* 876, 67. doi:10.3847/1538-4357/ab153a, arXiv:1904.02022.
- Bergeron, P., Kilic, M., Blouin, S., Bédard, A., Leggett, S.K., Brown, W.R., 2022. On the Nature of Ultracool White Dwarfs: Not so Cool after All. *ApJ* 934, 36. doi:10.3847/1538-4357/ac76c7, arXiv:2206.03174.

- Bergeron, P., Leggett, S.K., Ruiz, M.T., 2001. Photometric and Spectroscopic Analysis of Cool White Dwarfs with Trigonometric Parallax Measurements. *ApJS* 133, 413–449. doi:10.1086/320356, arXiv:astro-ph/0011286.
- Bergeron, P., Wesemael, F., Fontaine, G., 1992. On the Influence of the Convective Efficiency on the Determination of the Atmospheric Parameters of DA White Dwarfs. *ApJ* 387, 288. doi:10.1086/171080.
- Blouin, S., Bédard, A., Tremblay, P.E., 2023a. Carbon dredge-up required to explain the Gaia white dwarf colour-magnitude bifurcation. *MNRAS* doi:10.1093/mnras/stad1574, arXiv:2305.02827.
- Blouin, S., Daligault, J., 2021. Phase Separation in Ultramassive White Dwarfs. *ApJ* 919, 87. doi:10.3847/1538-4357/ac1513, arXiv:2107.07094.
- Blouin, S., Daligault, J., Saumon, D., 2021.  $^{22}\text{Ne}$  Phase Separation as a Solution to the Ultramassive White Dwarf Cooling Anomaly. *ApJL* 911, L5. doi:10.3847/2041-8213/abf14b, arXiv:2103.12892.
- Blouin, S., Daligault, J., Saumon, D., Bédard, A., Brassard, P., 2020. Toward precision cosmochronology. A new C/O phase diagram for white dwarfs. *A&A* 640, L11. doi:10.1051/0004-6361/202038879, arXiv:2007.13669.
- Blouin, S., Dufour, P., 2019. The evolution of carbon-polluted white dwarfs at low effective temperatures. *MNRAS* 490, 4166–4174. doi:10.1093/mnras/stz2915, arXiv:1910.06168.
- Blouin, S., Dufour, P., Allard, N.F., Salim, S., Rich, R.M., Koopmans, L.V.E., 2019a. A New Generation of Cool White Dwarf Atmosphere Models. III. WD J2356-209: Accretion of a Planetesimal with an Unusual Composition. *ApJ* 872, 188. doi:10.3847/1538-4357/ab0081, arXiv:1902.03219.
- Blouin, S., Dufour, P., Thibeault, C., Allard, N.F., 2019b. A New Generation of Cool White Dwarf Atmosphere Models. IV. Revisiting the Spectral Evolution of Cool White Dwarfs. *ApJ* 878, 63. doi:10.3847/1538-4357/ab1f82, arXiv:1905.02174.

- Blouin, S., Kilic, M., Bédard, A., Tremblay, P.E., 2023b. The ubiquity of carbon dredge-up in hydrogen-deficient white dwarfs as revealed by GALEX. *MNRAS* 525, L112–L116. doi:10.1093/mnrasl/slad105, arXiv:2307.14295.
- Blouin, S., Xu, S., 2022. No evidence for a strong decrease of planetesimal accretion in old white dwarfs. *MNRAS* 510, 1059–1067. doi:10.1093/mnras/stab3446, arXiv:2111.12152.
- Bohlin, R.C., Deustua, S.E., de Rosa, G., 2019. Hubble Space Telescope Flux Calibration. I. STIS and CALSPEC. *AJ* 158, 211. doi:10.3847/1538-3881/ab480c.
- Bohlin, R.C., Gordon, K.D., Tremblay, P.E., 2014. Techniques and Review of Absolute Flux Calibration from the Ultraviolet to the Mid-Infrared. *PASP* 126, 711. doi:10.1086/677655, arXiv:1406.1707.
- Braithwaite, J., Spruit, H.C., 2004. A fossil origin for the magnetic field in A stars and white dwarfs. *Nature* 431, 819–821. doi:10.1038/nature02934, arXiv:astro-ph/0502043.
- Brown, W.R., Kilic, M., Bédard, A., Kosakowski, A., Bergeron, P., 2020. A 1201 s Orbital Period Detached Binary: The First Double Helium Core White Dwarf LISA Verification Binary. *ApJL* 892, L35. doi:10.3847/2041-8213/ab8228, arXiv:2004.00641.
- Brown, W.R., Kilic, M., Kosakowski, A., Gianninas, A., 2022. The ELM Survey. IX. A Complete Sample of Low-mass White Dwarf Binaries in the SDSS Footprint. *ApJ* 933, 94. doi:10.3847/1538-4357/ac72ac, arXiv:2207.02998.
- Burdge, K. B. et al., 2022. A dense 0.1-solar-mass star in a 51-minute-orbital-period eclipsing binary. *Nature* 610, 467–471. doi:10.1038/s41586-022-05195-x, arXiv:2210.01809.
- Caiazzo, I. et al., 2023. A rotating white dwarf shows different compositions on its opposite faces. *Nature* 620, 61–66. doi:10.1038/s41586-023-06171-9, arXiv:2308.07430.



- Caiazzo, I. et al., 2020. Intermediate-mass Stars Become Magnetic White Dwarfs. *ApJL* 901, L14. doi:10.3847/2041-8213/abb5f7, arXiv:2009.03374.
- Camisassa, M., Torres, S., Hollands, M., Koester, D., Raddi, R., Althaus, L.G., Rebassa-Mansergas, A., 2023. A hidden population of white dwarfs with atmospheric carbon traces in the Gaia bifurcation. *A&A* 674, A213. doi:10.1051/0004-6361/202346628, arXiv:2305.02110.
- Camisassa, M.E., Althaus, L.G., Torres, S., Córscico, A.H., Rebassa-Mansergas, A., Tremblay, P.E., Cheng, S., Raddi, R., 2021. Forever young white dwarfs: When stellar ageing stops. *A&A* 649, L7. doi:10.1051/0004-6361/202140720, arXiv:2008.03028.
- Canbay, R., Bilir, S., Özdönmez, A., Ak, T., 2023. Galactic Model Parameters and Spatial Density of Cataclysmic Variables in the Gaia Era: New Constraints on Population Models. *AJ* 165, 163. doi:10.3847/1538-3881/acbead, arXiv:2302.11568.
- Caplan, M.E., Freeman, I.F., Horowitz, C.J., Cumming, A., Bellinger, E.P., 2021. Cooling Delays from Iron Sedimentation and Iron Inner Cores in White Dwarfs. *ApJL* 919, L12. doi:10.3847/2041-8213/ac1f99, arXiv:2108.11389.
- Caplan, M.E., Horowitz, C.J., Cumming, A., 2020. Neon Cluster Formation and Phase Separation during White Dwarf Cooling. *ApJL* 902, L44. doi:10.3847/2041-8213/abbd0, arXiv:2010.00036.
- Caron, A., Bergeron, P., Blouin, S., Leggett, S.K., 2023. A spectrophotometric analysis of cool white dwarfs in the Gaia and pan-STARRS footprint. *MNRAS* 519, 4529–4549. doi:10.1093/mnras/stac3733, arXiv:2212.08014.
- Cheng, S., Cummings, J.D., Ménard, B., 2019. A Cooling Anomaly of High-mass White Dwarfs. *ApJ* 886, 100. doi:10.3847/1538-4357/ab4989, arXiv:1905.12710.
- Cheng, S., Cummings, J.D., Ménard, B., Toonen, S., 2020. Double White Dwarf Merger Products among High-mass White Dwarfs. *ApJ* 891, 160. doi:10.3847/1538-4357/ab733c, arXiv:1910.09558.

- Cooper, A. P. et al., 2022. Overview of the DESI Milky Way Survey. arXiv e-prints , arXiv:2208.08514arXiv:2208.08514.
- Coutu, S., Dufour, P., Bergeron, P., Blouin, S., Loranger, E., Allard, N.F., Dunlap, B.H., 2019. Analysis of Helium-rich White Dwarfs Polluted by Heavy Elements in the Gaia Era. *ApJ* 885, 74. doi:10.3847/1538-4357/ab46b9, arXiv:1907.05932.
- Cukanovaite, E., Tremblay, P.E., Bergeron, P., Freytag, B., Ludwig, H.G., Steffen, M., 2021. 3D spectroscopic analysis of helium-line white dwarfs. *MNRAS* 501, 5274–5293. doi:10.1093/mnras/staa3684, arXiv:2011.12693.
- Cukanovaite, E., Tremblay, P.E., Toonen, S., Temmink, K.D., Manser, C.J., O’Brien, M.W., McCleery, J., 2023. Local stellar formation history from the 40 pc white dwarf sample. *MNRAS* 522, 1643–1661. doi:10.1093/mnras/stad1020, arXiv:2209.13919.
- Culpan, R., Geier, S., Reindl, N., Pelisoli, I., Gentile Fusillo, N., Vorontseva, A., 2022. The population of hot subdwarf stars studied with Gaia. IV. Catalogues of hot subluminous stars based on Gaia EDR3. *A&A* 662, A40. doi:10.1051/0004-6361/202243337, arXiv:2203.07938.
- Cunningham, T., Tremblay, P.E., Gentile Fusillo, N.P., Hollands, M., Cukanovaite, E., 2020. From hydrogen to helium: the spectral evolution of white dwarfs as evidence for convective mixing. *MNRAS* 492, 3540–3552. doi:10.1093/mnras/stz3638, arXiv:1911.00014.
- Cunningham, T., Tremblay, P.E., W. O’Brien, M., 2024. Initial-final mass relation from white dwarfs within 40 pc. *MNRAS* 527, 3602–3611. doi:10.1093/mnras/stad3275, arXiv:2310.15410.
- de Jong, R. S. et al., 2019. 4MOST: Project overview and information for the First Call for Proposals. *The Messenger* 175, 3–11. doi:10.18727/0722-6691/5117, arXiv:1903.02464.
- Dickson, N., Hénault-Brunet, V., Baumgardt, H., Gieles, M., Smith, P.J., 2023. Multimass modelling of Milky Way globular clusters - I. Implications on their stellar initial mass function above  $1 M_{\odot}$ . *MNRAS* 522, 5320–5339. doi:10.1093/mnras/stad1254, arXiv:2303.01637.

- Doyle, A. E. et al., 2023. New Chondritic Bodies Identified in Eight Oxygen-bearing White Dwarfs. *ApJ* 950, 93. doi:10.3847/1538-4357/acbd44, arXiv:2303.00063.
- El-Badry, K., 2024. Gaia’s binary star renaissance. arXiv e-prints , arXiv:2403.12146doi:10.48550/arXiv.2403.12146, arXiv:2403.12146.
- El-Badry, K., Rix, H.W., Heintz, T.M., 2021a. A million binaries from Gaia eDR3: sample selection and validation of Gaia parallax uncertainties. *MNRAS* 506, 2269–2295. doi:10.1093/mnras/stab323, arXiv:2101.05282.
- El-Badry, K., Rix, H.W., Quataert, E., Kupfer, T., Shen, K.J., 2021b. Birth of the ELMs: a ZTF survey for evolved cataclysmic variables turning into extremely low-mass white dwarfs. *MNRAS* 508, 4106–4139. doi:10.1093/mnras/stab2583, arXiv:2108.04255.
- El-Badry, K., Rix, H.W., Weisz, D.R., 2018. An Empirical Measurement of the Initial-Final Mass Relation with Gaia White Dwarfs. *ApJL* 860, L17. doi:10.3847/2041-8213/aaca9c, arXiv:1805.05849.
- El-Badry, K. et al., 2023. The fastest stars in the Galaxy. *The Open Journal of Astrophysics* 6, 28. doi:10.21105/astro.2306.03914, arXiv:2306.03914.
- Elms, A.K., Tremblay, P.E., Gänsicke, B.T., Koester, D., Hollands, M.A., Gentile Fusillo, N.P., Cunningham, T., Apps, K., 2022. Spectral analysis of ultra-cool white dwarfs polluted by planetary debris. *MNRAS* 517, 4557–4574. doi:10.1093/mnras/stac2908, arXiv:2206.05258.
- Elms, A. K. et al., 2023. An emerging and enigmatic spectral class of isolated DAe white dwarfs. *MNRAS* 524, 4996–5015. doi:10.1093/mnras/stad2171, arXiv:2307.09186.
- Fantin, N.J., Côté, P., McConnachie, A.W., 2020. White Dwarfs in the Era of the LSST and Its Synergies with Space-based Missions. *ApJ* 900, 139. doi:10.3847/1538-4357/aba270, arXiv:2007.01312.
- Fantin, N. J. et al., 2021. The Mass and Age Distribution of Halo White Dwarfs in the Canada-France Imaging Survey. *ApJ* 913, 30. doi:10.3847/1538-4357/abf2b2, arXiv:2103.14721.

- Fantin, N. J. et al., 2019. The Canada-France Imaging Survey: Reconstructing the Milky Way Star Formation History from Its White Dwarf Population. *ApJ* 887, 148. doi:10.3847/1538-4357/ab5521, arXiv:1911.02576.
- Farihi, J., 2016. Circumstellar debris and pollution at white dwarf stars. *New Astronomy Reviews* 71, 9–34. doi:10.1016/j.newar.2016.03.001, arXiv:1604.03092.
- Farihi, J., Hermes, J.J., Littlefair, S.P., Howarth, I.D., Walters, N., Parsons, S.G., 2023. Discovery of dipolar chromospheres in two white dwarfs. *MNRAS* 525, 1097–1105. doi:10.1093/mnras/stad2184, arXiv:2307.02543.
- Ferrario, L., Wickramasinghe, D., Kawka, A., 2020. Magnetic fields in isolated and interacting white dwarfs. *Advances in Space Research* 66, 1025–1056. doi:10.1016/j.asr.2019.11.012, arXiv:2001.10147.
- Fleury, L., Caiazzo, I., Heyl, J., 2022. The cooling of massive white dwarfs from Gaia EDR3. *MNRAS* 511, 5984–5993. doi:10.1093/mnras/stac458, arXiv:2110.00598.
- Fontaine, G., Brassard, P., Bergeron, P., 2001. The Potential of White Dwarf Cosmochronology. *PASP* 113, 409–435. doi:10.1086/319535.
- Fouesneau, M., Rix, H.W., von Hippel, T., Hogg, D.W., Tian, H., 2019. Precise Ages of Field Stars from White Dwarf Companions. *ApJ* 870, 9. doi:10.3847/1538-4357/aaee74, arXiv:1802.06663.
- Fuentes, J.R., Castro-Tapia, M., Cumming, A., 2024. A Short Intense Dynamo at the Onset of Crystallization in White Dwarfs. *ApJL* 964, L15. doi:10.3847/2041-8213/ad3100, arXiv:2402.03639.
- Gagné, J., David, T.J., Mamajek, E.E., Mann, A.W., Faherty, J.K., Bédard, A., 2020. The  $\mu$  Tau Association: A 60 Myr Old Coeval Group at 150 pc from the Sun. *ApJ* 903, 96. doi:10.3847/1538-4357/abb77e, arXiv:2008.06139.
- Gaia Collaboration et al., 2018. Gaia Data Release 2. Observational Hertzsprung-Russell diagrams. *A&A* 616, A10. doi:10.1051/0004-6361/201832843, arXiv:1804.09378.

- Gaia Collaboration et al., 2023a. Gaia Data Release 3. The Galaxy in your preferred colours: Synthetic photometry from Gaia low-resolution spectra. *A&A* 674, A33. doi:10.1051/0004-6361/202243709, arXiv:2206.06215.
- Gaia Collaboration et al., 2016. The Gaia mission. *A&A* 595, A1. doi:10.1051/0004-6361/201629272, arXiv:1609.04153.
- Gaia Collaboration et al., 2021. Gaia Early Data Release 3. The Gaia Catalogue of Nearby Stars. *A&A* 649, A6. doi:10.1051/0004-6361/202039498, arXiv:2012.02061.
- Gaia Collaboration et al., 2023b. Gaia Data Release 3. Summary of the content and survey properties. *A&A* 674, A1. doi:10.1051/0004-6361/202243940, arXiv:2208.00211.
- Gänsicke, B.T., Rodríguez-Gil, P., Gentile Fusillo, N.P., Inight, K., Schreiber, M.R., Pala, A.F., Tremblay, P.E., 2020. Single magnetic white dwarfs with Balmer emission lines: a small class with consistent physical characteristics as possible signposts for close-in planetary companions. *MNRAS* 499, 2564–2574. doi:10.1093/mnras/staa2969, arXiv:2009.11925.
- Garbutt, J. A. et al., 2024. The white dwarf binary pathways survey - X. Gaia orbits for known UV excess binaries. *MNRAS* 529, 4840–4855. doi:10.1093/mnras/stae807, arXiv:2403.07985.
- García-Berro, E. et al., 2012. Double Degenerate Mergers as Progenitors of High-field Magnetic White Dwarfs. *ApJ* 749, 25. doi:10.1088/0004-637X/749/1/25, arXiv:1202.0461.
- García-Zamora, E.M., Torres, S., Rebassa-Mansergas, A., 2023. White dwarf Random Forest classification through Gaia spectral coefficients. *A&A* 679, A127. doi:10.1051/0004-6361/202347601, arXiv:2308.07090.
- Genest-Beaulieu, C., Bergeron, P., 2019a. A Comprehensive Spectroscopic and Photometric Analysis of DA and DB White Dwarfs from SDSS and Gaia. *ApJ* 871, 169. doi:10.3847/1538-4357/aafac6.
- Genest-Beaulieu, C., Bergeron, P., 2019b. A Photometric and Spectroscopic Investigation of the DB White Dwarf Population Using SDSS and Gaia Data. *ApJ* 882, 106. doi:10.3847/1538-4357/ab379e, arXiv:1908.01728.

- Gentile Fusillo, N. P. et al., 2021a. White dwarfs with planetary remnants in the era of Gaia - I. Six emission line systems. *MNRAS* 504, 2707–2726. doi:10.1093/mnras/stab992, arXiv:2010.13807.
- Gentile Fusillo, N.P., Tremblay, P.E., Bohlin, R.C., Deustua, S.E., Kalirai, J.S., 2020. Cool white dwarfs as standards for infrared observations. *MNRAS* 491, 3613–3623. doi:10.1093/mnras/stz2984, arXiv:1910.08087.
- Gentile Fusillo, N. P. et al., 2021b. A catalogue of white dwarfs in Gaia EDR3. *MNRAS* 508, 3877–3896. doi:10.1093/mnras/stab2672, arXiv:2106.07669.
- Gentile Fusillo, N. P. et al., 2019. A Gaia Data Release 2 catalogue of white dwarfs and a comparison with SDSS. *MNRAS* 482, 4570–4591. doi:10.1093/mnras/sty3016, arXiv:1807.03315.
- Giammichele, N., Bergeron, P., Dufour, P., 2012. Know Your Neighborhood: A Detailed Model Atmosphere Analysis of Nearby White Dwarfs. *ApJS* 199, 29. doi:10.1088/0067-0049/199/2/29, arXiv:1202.5581.
- Gianninas, A., Bergeron, P., Ruiz, M.T., 2011. A Spectroscopic Survey and Analysis of Bright, Hydrogen-rich White Dwarfs. *ApJ* 743, 138. doi:10.1088/0004-637X/743/2/138, arXiv:1109.3171.
- Ginzburg, S., Fuller, J., Kawka, A., Caiazzo, I., 2022. Slow convection and fast rotation in crystallization-driven white dwarf dynamos. *MNRAS* 514, 4111–4119. doi:10.1093/mnras/stac1363, arXiv:2202.12902.
- Golovin, A., Reffert, S., Vani, A., Bastian, U., Jordan, S., Just, A., 2024. Identification of new nearby white dwarfs using Gaia DR3. *A&A* 683, A33. doi:10.1051/0004-6361/202347767, arXiv:2312.11664.
- Griggio, M. et al., 2022. Astro-photometric study of M37 with Gaia and wide-field ugi-imaging. *MNRAS* 515, 1841–1853. doi:10.1093/mnras/stac1920, arXiv:2207.03179.
- Guidry, J. A. et al., 2021. I Spy Transits and Pulsations: Empirical Variability in White Dwarfs Using Gaia and the Zwicky Transient Facility. *ApJ* 912, 125. doi:10.3847/1538-4357/abee68, arXiv:2012.00035.

- Hardy, F., Dufour, P., Jordan, S., 2023a. Spectrophotometric analysis of magnetic white dwarf - I. Hydrogen-rich compositions. *MNRAS* 520, 6111–6134. doi:10.1093/mnras/stad196, arXiv:2301.06596.
- Hardy, F., Dufour, P., Jordan, S., 2023b. Spectrophotometric analysis of magnetic white dwarf - I. Hydrogen-rich compositions. *MNRAS* 520, 6111–6134. doi:10.1093/mnras/stad196, arXiv:2301.06596.
- Heintz, T.M., Hermes, J.J., El-Badry, K., Walsh, C., van Saders, J.L., Fields, C.E., Koester, D., 2022. Testing White Dwarf Age Estimates Using Wide Double White Dwarf Binaries from Gaia EDR3. *ApJ* 934, 148. doi:10.3847/1538-4357/ac78d9, arXiv:2206.00025.
- Heintz, T.M., Hermes, J.J., Tremblay, P.E., Baya Ould Rouis, L., Redding, J.S., Kaiser, B.C., van Saders, J.L., 2024. A Test of Spectroscopic Age Estimates of White Dwarfs using Wide WD+WD Binaries. arXiv e-prints, arXiv:2405.02423doi:10.48550/arXiv.2405.02423, arXiv:2405.02423.
- Heyl, J., Caiazzo, I., Richer, H.B., 2022. Reconstructing the Pleiades with Gaia EDR3. *ApJ* 926, 132. doi:10.3847/1538-4357/ac45fc, arXiv:2110.03837.
- Hodgkin, S. T. et al., 2021. Gaia Early Data Release 3. Gaia photometric science alerts. *A&A* 652, A76. doi:10.1051/0004-6361/202140735, arXiv:2106.01394.
- Holberg, J.B., Oswalt, T.D., Sion, E.M., McCook, G.P., 2016. The 25 parsec local white dwarf population. *MNRAS* 462, 2295–2318. doi:10.1093/mnras/stw1357.
- Hollands, M.A., Littlefair, S.P., Parsons, S.G., 2024. Measuring the initial-final mass relation using wide double white dwarf binaries from Gaia DR3. *MNRAS* 527, 9061–9117. doi:10.1093/mnras/stad3729, arXiv:2311.14801.
- Hollands, M. A. et al., 2020. An ultra-massive white dwarf with a mixed hydrogen-carbon atmosphere as a likely merger remnant. *Nature Astronomy* 4, 663–669. doi:10.1038/s41550-020-1028-0, arXiv:2003.00028.

- Hollands, M.A., Tremblay, P.E., Gänsicke, B.T., Gentile-Fusillo, N.P., Toonen, S., 2018. The Gaia 20 pc white dwarf sample. *MNRAS* 480, 3942–3961. doi:10.1093/mnras/sty2057, arXiv:1805.12590.
- Hollands, M.A., Tremblay, P.E., Gänsicke, B.T., Koester, D., 2022. Spectral analysis of cool white dwarfs accreting from planetary systems: from the ultraviolet to the optical. *MNRAS* 511, 71–82. doi:10.1093/mnras/stab3696, arXiv:2112.08887.
- Hollands, M.A., Tremblay, P.E., Gänsicke, B.T., Koester, D., Gentile-Fusillo, N.P., 2021. Alkali metals in white dwarf atmospheres as tracers of ancient planetary crusts. *Nature Astronomy* 5, 451–459. doi:10.1038/s41550-020-01296-7, arXiv:2101.01225.
- Horowitz, C.J., 2020. Nuclear and dark matter heating in massive white dwarf stars. *PhRvD* 102, 083031. doi:10.1103/PhysRevD.102.083031, arXiv:2008.03291.
- Hwang, H.C., Ting, Y.S., Cheng, S., Speagle, J.S., 2024. Dynamical masses across the Hertzsprung-Russell diagram. *MNRAS* 528, 4272–4288. doi:10.1093/mnras/stae297, arXiv:2308.08584.
- Igoshev, A.P., Perets, H., Hallakoun, N., 2023. Hyper-runaway and hypervelocity white dwarf candidates in Gaia Data Release 3: Possible remnants from Ia/Iax supernova explosions or dynamical encounters. *MNRAS* 518, 6223–6237. doi:10.1093/mnras/stac3488, arXiv:2209.09915.
- Inight, K., Gänsicke, B.T., Breedt, E., Marsh, T.R., Pala, A.F., Raddi, R., 2021. Towards a volumetric census of close white dwarf binaries - I. Reference samples. *MNRAS* 504, 2420–2442. doi:10.1093/mnras/stab753, arXiv:2103.06892.
- Inight, K. et al., 2023. Cataclysmic Variables from Sloan Digital Sky Survey - V. The search for period bouncers continues. *MNRAS* 525, 3597–3625. doi:10.1093/mnras/stad2409, arXiv:2305.13371.
- Isern, J., 2019. The Star Formation History in the Solar Neighborhood as Told by Massive White Dwarfs. *ApJL* 878, L11. doi:10.3847/2041-8213/ab238e, arXiv:1905.10779.



- Isern, J., García-Berro, E., Külebi, B., Lorén-Aguilar, P., 2017. A Common Origin of Magnetism from Planets to White Dwarfs. *ApJL* 836, L28. doi:10.3847/2041-8213/aa5eae, arXiv:1702.01813.
- Izquierdo, P., Gänsicke, B.T., Rodríguez-Gil, P., Koester, D., Toloza, O., Gentile Fusillo, N.P., Pala, A.F., Tremblay, P.E., 2023. Systematic uncertainties in the characterization of helium-dominated metal-polluted white dwarf atmospheres. *MNRAS* 520, 2843–2866. doi:10.1093/mnras/stad282, arXiv:2301.09670.
- Izquierdo, P., Toloza, O., Gänsicke, B.T., Rodríguez-Gil, P., Farihi, J., Koester, D., Guo, J., Redfield, S., 2021. GD 424 - a helium-atmosphere white dwarf with a large amount of trace hydrogen in the process of digesting a rocky planetesimal. *MNRAS* 501, 4276–4288. doi:10.1093/mnras/staa3987, arXiv:2012.12957.
- Jiménez-Esteban, F.M., Torres, S., Rebassa-Mansergas, A., Cruz, P., Murillo-Ojeda, R., Solano, E., Rodrigo, C., Camisassa, M.E., 2023. Spectral classification of the 100 pc white dwarf population from Gaia-DR3 and the virtual observatory. *MNRAS* 518, 5106–5122. doi:10.1093/mnras/stac3382, arXiv:2211.08852.
- Jiménez-Esteban, F.M., Torres, S., Rebassa-Mansergas, A., Skorobogatov, G., Solano, E., Cantero, C., Rodrigo, C., 2018. A white dwarf catalogue from Gaia-DR2 and the Virtual Observatory. *MNRAS* 480, 4505–4518. doi:10.1093/mnras/sty2120, arXiv:1807.02559.
- Jin, S. et al., 2024. The wide-field, multiplexed, spectroscopic facility WEAVE: Survey design, overview, and simulated implementation. *MNRAS* 530, 2688–2730. doi:10.1093/mnras/stad557, arXiv:2212.03981.
- Johnson, T.M., Klein, B.L., Koester, D., Melis, C., Zuckerman, B., Jura, M., 2022. Unusual Abundances from Planetary System Material Polluting the White Dwarf G238-44. *ApJ* 941, 113. doi:10.3847/1538-4357/aca089, arXiv:2211.02673.
- Joyce, S.R.G., Barstow, M.A., Casewell, S.L., Burleigh, M.R., Holberg, J.B., Bond, H.E., 2018. Testing the white dwarf mass-radius relation and comparing optical and far-UV spectroscopic results with Gaia DR2,

- HST, and FUSE. *MNRAS* 479, 1612–1626. doi:10.1093/mnras/sty1425, arXiv:1806.00061.
- Jura, M., 2003. A Tidally Disrupted Asteroid around the White Dwarf G29-38. *ApJL* 584, L91–L94. doi:10.1086/374036, arXiv:astro-ph/0301411.
- Kaiser, B.C., Clemens, J.C., Blouin, S., Dufour, P., Hegedus, R.J., Reding, J.S., Bédard, A., 2021. Lithium pollution of a white dwarf records the accretion of an extrasolar planetesimal. *Science* 371, 168–172. doi:10.1126/science.abd1714, arXiv:2012.12900.
- Kawash, A. et al., 2022. The Galactic Nova Rate: Estimates from the ASAS-SN and Gaia Surveys. *ApJ* 937, 64. doi:10.3847/1538-4357/ac8d5e, arXiv:2206.14132.
- Kawka, A., Ferrario, L., Vennes, S., 2023. The non-explosive stellar merging origin of the ultra-massive carbon-rich white dwarfs. *MNRAS* 520, 6299–6311. doi:10.1093/mnras/stad553, arXiv:2302.11118.
- Kawka, A., Simpson, J.D., Vennes, S., Bessell, M.S., Da Costa, G.S., Marino, A.F., Murphy, S.J., 2020. The closest extremely low-mass white dwarf to the Sun. *MNRAS* 495, L129–L134. doi:10.1093/mnrasl/slaa068, arXiv:2004.07556.
- Keller, P.M., Breedt, E., Hodgkin, S., Belokurov, V., Wild, J., García-Soriano, I., Wise, J.L., 2022. Eclipsing white dwarf binaries in Gaia and the Zwicky Transient Facility. *MNRAS* 509, 4171–4188. doi:10.1093/mnras/stab3293, arXiv:2105.14028.
- Kepler, S. O. et al., 2019. White dwarf and subdwarf stars in the Sloan Digital Sky Survey Data Release 14. *MNRAS* 486, 2169–2183. doi:10.1093/mnras/stz960, arXiv:1904.01626.
- Kervella, P., Arenou, F., Thévenin, F., 2022. Stellar and substellar companions from Gaia EDR3. Proper-motion anomaly and resolved common proper-motion pairs. *A&A* 657, A7. doi:10.1051/0004-6361/202142146, arXiv:2109.10912.
- Kilic, M., Bédard, A., Bergeron, P., 2021a. Hidden in plain sight: a double-lined white dwarf binary 26 pc away and a distant cousin. *MNRAS* 502, 4972–4980. doi:10.1093/mnras/stab439, arXiv:2102.05688.

- Kilic, M., Bédard, A., Bergeron, P., Kosakowski, A., 2020a. Two new double-lined spectroscopic binary white dwarfs. *MNRAS* 493, 2805–2816. doi:10.1093/mnras/staa466, arXiv:2002.06214.
- Kilic, M., Bergeron, P., Blouin, S., Jewett, G., Brown, W.R., Moss, A., 2024. White Dwarf Merger Remnants: The DAQ Subclass. *ApJ* 965, 159. doi:10.3847/1538-4357/ad3440, arXiv:2403.08878.
- Kilic, M., Bergeron, P., Dame, K., Hambly, N.C., Rowell, N., Crawford, C.L., 2019. The age of the Galactic stellar halo from Gaia white dwarfs. *MNRAS* 482, 965–979. doi:10.1093/mnras/sty2755, arXiv:1810.03536.
- Kilic, M., Bergeron, P., Kosakowski, A., Brown, W.R., Agüeros, M.A., Blouin, S., 2020b. The 100 pc White Dwarf Sample in the SDSS Footprint. *ApJ* 898, 84. doi:10.3847/1538-4357/ab9b8d, arXiv:2006.00323.
- Kilic, M., Brown, W.R., Bédard, A., Kosakowski, A., 2021b. The Discovery of Two LISA Sources within 0.5 kpc. *ApJL* 918, L14. doi:10.3847/2041-8213/ac1e2b, arXiv:2108.08324.
- Kilic, M. et al., 2023. The merger fraction of ultramassive white dwarfs. *MNRAS* 518, 2341–2353. doi:10.1093/mnras/stac3182, arXiv:2211.05938.
- Kirkpatrick, J. D. et al., 2024. The Initial Mass Function Based on the Full-sky 20 pc Census of  $\sim 3600$  Stars and Brown Dwarfs. *ApJS* 271, 55. doi:10.3847/1538-4365/ad24e2, arXiv:2312.03639.
- Kissin, Y., Thompson, C., 2015. Spin and Magnetism of White Dwarfs. *ApJ* 809, 108. doi:10.1088/0004-637X/809/2/108, arXiv:1501.07197.
- Klein, B.L., Doyle, A.E., Zuckerman, B., Dufour, P., Blouin, S., Melis, C., Weinberger, A.J., Young, E.D., 2021. Discovery of Beryllium in White Dwarfs Polluted by Planetesimal Accretion. *ApJ* 914, 61. doi:10.3847/1538-4357/abe40b, arXiv:2102.01834.
- Koester, D., Kepler, S.O., 2019. Carbon-rich (DQ) white dwarfs in the Sloan Digital Sky Survey. *A&A* 628, A102. doi:10.1051/0004-6361/201935946, arXiv:1905.11174.
- Koester, D., Kepler, S.O., Irwin, A.W., 2020. New white dwarf envelope models and diffusion. Application to DQ white dwarfs. *A&A* 635, A103. doi:10.1051/0004-6361/202037530, arXiv:2002.10170.

- Koester, D., Schulz, H., Weidemann, V., 1979. Atmospheric parameters and mass distribution of DA white dwarfs. *A&A* 76, 262–275.
- Kollmeier, J. A. et al., 2017. SDSS-V: Pioneering Panoptic Spectroscopy. *arXiv e-prints*, arXiv:1711.03234doi:10.48550/arXiv.1711.03234, arXiv:1711.03234.
- Korol, V., Belokurov, V., Toonen, S., 2022. A gap in the double white dwarf separation distribution caused by the common-envelope evolution: astrometric evidence from Gaia. *MNRAS* 515, 1228–1246. doi:10.1093/mnras/stac1686, arXiv:2203.03659.
- Kosakowski, A., Brown, W.R., Kilic, M., Kupfer, T., Bédard, A., Gianninas, A., Agüeros, M.A., Barrientos, M., 2023. The ELM Survey South. II. Two Dozen New Low-mass White Dwarf Binaries. *ApJ* 950, 141. doi:10.3847/1538-4357/acd187, arXiv:2305.03079.
- Kupfer, T. et al., 2024. LISA Galactic Binaries with Astrometry from Gaia DR3. *ApJ* 963, 100. doi:10.3847/1538-4357/ad2068, arXiv:2302.12719.
- Lai, S. et al., 2021. Infrared Excesses Around Bright White Dwarfs from Gaia and unWISE. II. *ApJ* 920, 156. doi:10.3847/1538-4357/ac1354, arXiv:2107.01221.
- Lamberts, A., Blunt, S., Littenberg, T.B., Garrison-Kimmel, S., Kupfer, T., Sanderson, R.E., 2019. Predicting the LISA white dwarf binary population in the Milky Way with cosmological simulations. *MNRAS* 490, 5888–5903. doi:10.1093/mnras/stz2834, arXiv:1907.00014.
- Landstreet, J.D., Bagnulo, S., 2019. A new weak-field magnetic DA white dwarf in the local 20 pc volume. The frequency of magnetic fields in DA stars. *A&A* 628, A1. doi:10.1051/0004-6361/201936009, arXiv:1907.01626.
- Leggett, S. K. et al., 2018. Distant White Dwarfs in the US Naval Observatory Flagstaff Station Parallax Sample. *ApJS* 239, 26. doi:10.3847/1538-4365/aae7ca, arXiv:1809.10803.
- Limoges, M.M., Bergeron, P., Lépine, S., 2015. Physical Properties of the Current Census of Northern White Dwarfs within 40 pc of the Sun. *ApJS* 219, 19. doi:10.1088/0067-0049/219/2/19, arXiv:1505.02297.

- Lindgren, L., Dravins, D., 2021. Astrometric radial velocities for nearby stars. *A&A* 652, A45. doi:10.1051/0004-6361/202141344, arXiv:2105.09014.
- Lodieu, N., Pérez-Garrido, A., Smart, R.L., Silvotti, R., 2019a. A 5D view of the  $\alpha$  Per, Pleiades, and Praesepe clusters. *A&A* 628, A66. doi:10.1051/0004-6361/201935533, arXiv:1906.03924.
- Lodieu, N., Smart, R.L., Pérez-Garrido, A., Silvotti, R., 2019b. A 3D view of the Hyades stellar and sub-stellar population. *A&A* 623, A35. doi:10.1051/0004-6361/201834045, arXiv:1901.07534.
- López-Sanjuan, C. et al., 2022. J-PLUS: Spectral evolution of white dwarfs by PDF analysis. *A&A* 658, A79. doi:10.1051/0004-6361/202141746, arXiv:2110.14421.
- López-Sanjuan, C. et al., 2019. J-PLUS: photometric calibration of large-area multi-filter surveys with stellar and white dwarf loci. *A&A* 631, A119. doi:10.1051/0004-6361/201936405, arXiv:1907.12939.
- Maíz Apellániz, J., Weiler, M., 2018. Reanalysis of the Gaia Data Release 2 photometric sensitivity curves using HST/STIS spectrophotometry. *A&A* 619, A180. doi:10.1051/0004-6361/201834051, arXiv:1808.02820.
- Manser, C.J., Gänsicke, B.T., Gentile Fusillo, N.P., Ashley, R., Breedt, E., Hollands, M., Izquierdo, P., Pelisoli, I., 2020. The frequency of gaseous debris discs around white dwarfs. *MNRAS* 493, 2127–2139. doi:10.1093/mnras/staa359, arXiv:2002.01936.
- Manser, C. J. et al., 2023. DAHe white dwarfs from the DESI Survey. *MNRAS* 521, 4976–4994. doi:10.1093/mnras/stad727, arXiv:2302.01335.
- Marigo, P. et al., 2020. Carbon star formation as seen through the non-monotonic initial-final mass relation. *Nature Astronomy* 4, 1102–1110. doi:10.1038/s41550-020-1132-1, arXiv:2007.04163.
- McCleery, J. et al., 2020. Gaia white dwarfs within 40 pc II: the volume-limited Northern hemisphere sample. *MNRAS* 499, 1890–1908. doi:10.1093/mnras/staa2030, arXiv:2006.00874.

- McGill, P. et al., 2023. First semi-empirical test of the white dwarf mass-radius relationship using a single white dwarf via astrometric microlensing. *MNRAS* 520, 259–280. doi:10.1093/mnras/stac3532, arXiv:2206.01814.
- McGill, P., Smith, L.C., Evans, N.W., Belokurov, V., Smart, R.L., 2018. A predicted astrometric microlensing event by a nearby white dwarf. *MNRAS* 478, L29–L33. doi:10.1093/mnrasl/sly066, arXiv:1804.07049.
- Melis, C., Klein, B., Doyle, A.E., Weinberger, A., Zuckerman, B., Dufour, P., 2020. Serendipitous Discovery of Nine White Dwarfs with Gaseous Debris Disks. *ApJ* 905, 56. doi:10.3847/1538-4357/abbdfa, arXiv:2010.03695.
- Mikkola, D., McMillan, P.J., Hobbs, D., Wimarsson, J., 2022. The velocity distribution of white dwarfs in Gaia EDR3. *MNRAS* 512, 6201–6216. doi:10.1093/mnras/stac434, arXiv:2202.07672.
- Miller, D.R., Caiazzo, I., Heyl, J., Richer, H.B., El-Badry, K., Rodriguez, A.C., Vanderbosch, Z.P., van Roestel, J., 2023. An Extremely Massive White Dwarf Escaped from the Hyades Star Cluster. *ApJL* 956, L41. doi:10.3847/2041-8213/acffc4, arXiv:2310.03204.
- Montgomery, M.H., Dunlap, B.H., 2024. Fluid Mixing during Phase Separation in Crystallizing White Dwarfs. *ApJ* 961, 197. doi:10.3847/1538-4357/ad16dc, arXiv:2312.11647.
- Moss, A. et al., 2022. Improving White Dwarfs as Chronometers with Gaia Parallaxes and Spectroscopic Metallicities. *ApJ* 929, 26. doi:10.3847/1538-4357/ac5ac0, arXiv:2203.08971.
- Munday, J. et al., 2023. An eclipsing 47 min double white dwarf binary at 400 pc. *MNRAS* 525, 1814–1823. doi:10.1093/mnras/stad2347, arXiv:2308.00036.
- Narayan, G. et al., 2019. Subpercent Photometry: Faint DA White Dwarf Spectrophotometric Standards for Astrophysical Observatories. *ApJS* 241, 20. doi:10.3847/1538-4365/ab0557, arXiv:1811.12534.
- Nayak, P.K., Ganguly, A., Chatterjee, S., 2023. Hunting Down White Dwarf-Main Sequence Binaries Using Multi-Wavelength Observations. *MNRAS* doi:10.1093/mnras/stad3580, arXiv:2212.09800.

- Noor, H.T., Farihi, J., Hollands, M., Toonen, S., 2024. White dwarf pollution: one star or two? *MNRAS* 529, 2910–2917. doi:10.1093/mnras/stae731, arXiv:2403.08870.
- O’Brien, M. W. et al., 2023. Gaia white dwarfs within 40 pc - III. Spectroscopic observations of new candidates in the Southern hemisphere. *MNRAS* 518, 3055–3073. doi:10.1093/mnras/stac3303, arXiv:2210.01608.
- O’Brien, M. W. et al., 2024. The 40 pc sample of white dwarfs from Gaia. *MNRAS* 527, 8687–8705. doi:10.1093/mnras/stad3773, arXiv:2312.02735.
- Ourique, G., Romero, A.D., Kepler, S.O., Koester, D., Amaral, L.A., 2019. A study of cool white dwarfs in the Sloan Digital Sky Survey Data Release 12. *MNRAS* 482, 649–657. doi:10.1093/mnras/sty2751, arXiv:1810.03554.
- Pala, A. F. et al., 2022. Constraining the evolution of cataclysmic variables via the masses and accretion rates of their underlying white dwarfs. *MNRAS* 510, 6110–6132. doi:10.1093/mnras/stab3449, arXiv:2111.13706.
- Pala, A. F. et al., 2020. A Volume-limited Sample of Cataclysmic Variables from Gaia DR2: Space Density and Population Properties. *MNRAS* 494, 3799–3827. doi:10.1093/mnras/staa764, arXiv:1907.13152.
- Parsons, S. G. et al., 2017. Testing the white dwarf mass-radius relationship with eclipsing binaries. *MNRAS* 470, 4473–4492. doi:10.1093/mnras/stx1522, arXiv:1706.05016.
- Pasquini, L., Pala, A.F., Salaris, M., Ludwig, H.G., Leão, I., Weiss, A., de Medeiros, J.R., 2023. Accurate mass-radius ratios for Hyades white dwarfs. *MNRAS* 522, 3710–3718. doi:10.1093/mnras/stad1252, arXiv:2304.10485.
- Pelisoli, I., Bell, K.J., Kepler, S.O., Koester, D., 2019. The sdA problem - III. New extremely low-mass white dwarfs and their precursors from Gaia astrometry. *MNRAS* 482, 3831–3842. doi:10.1093/mnras/sty2979, arXiv:1805.04070.
- Pelisoli, I., Vos, J., 2019. Gaia Data Release 2 catalogue of extremely low-mass white dwarf candidates. *MNRAS* 488, 2892–2903. doi:10.1093/mnras/stz1876, arXiv:1907.03766.

- Penoyre, Z., Belokurov, V., Evans, N.W., 2022. Astrometric identification of nearby binary stars - II. Astrometric binaries in the Gaia Catalogue of Nearby Stars. *MNRAS* 513, 5270–5289. doi:10.1093/mnras/stac1147, arXiv:2202.06963.
- Prišegen, M., Faltová, N., 2023. Uncovering new white dwarf-open cluster associations using Gaia DR3. *A&A* 678, A20. doi:10.1051/0004-6361/202245706, arXiv:2307.01337.
- Prišegen, M., Piecka, M., Faltová, N., Kajan, M., Paunzen, E., 2021. White dwarf-open cluster associations based on Gaia DR2. *A&A* 645, A13. doi:10.1051/0004-6361/202039276, arXiv:2011.03578.
- Qiu, D., Tian, H.J., Wang, X.D., Nie, J.L., von Hippel, T., Liu, G.C., Fouesneau, M., Rix, H.W., 2021. Precise Ages of Field Stars from White Dwarf Companions in Gaia DR2. *ApJS* 253, 58. doi:10.3847/1538-4365/abe468, arXiv:2012.04890.
- Raddi, R. et al., 2019. Partly burnt runaway stellar remnants from peculiar thermonuclear supernovae. *MNRAS* 489, 1489–1508. doi:10.1093/mnras/stz1618, arXiv:1902.05061.
- Raddi, R. et al., 2022. Kinematic properties of white dwarfs. Galactic orbital parameters and age-velocity dispersion relation. *A&A* 658, A22. doi:10.1051/0004-6361/202141837, arXiv:2111.01145.
- Ramsay, G. et al., 2018. Physical properties of AM CVn stars: New insights from Gaia DR2. *A&A* 620, A141. doi:10.1051/0004-6361/201834261, arXiv:1810.06548.
- Rebassa-Mansergas, A. et al., 2021a. Constraining the solar neighbourhood age-metallicity relation from white dwarf-main sequence binaries. *MNRAS* 505, 3165–3176. doi:10.1093/mnras/stab1559, arXiv:2105.13379.
- Rebassa-Mansergas, A. et al., 2023. Main-sequence companions to white dwarfs - II. The age-activity-rotation relation from a sample of Gaia common proper motion pairs. *MNRAS* 526, 4787–4800. doi:10.1093/mnras/stad3050, arXiv:2310.02125.



- Rebassa-Mansergas, A. et al., 2021b. White dwarf-main-sequence binaries from Gaia EDR3: the unresolved 100 pc volume-limited sample. *MNRAS* 506, 5201–5211. doi:10.1093/mnras/stab2039, arXiv:2107.06303.
- Rebassa-Mansergas, A., Solano, E., Xu, S., Rodrigo, C., Jiménez-Esteban, F.M., Torres, S., 2019. Infrared-excess white dwarfs in the Gaia 100 pc sample. *MNRAS* 489, 3990–4000. doi:10.1093/mnras/stz2423, arXiv:1908.11176.
- Reding, J.S., Hermes, J.J., Clemens, J.C., Hegedus, R.J., Kaiser, B.C., 2023. Two new white dwarfs with variable magnetic Balmer emission lines. *MNRAS* 522, 693–699. doi:10.1093/mnras/stad760, arXiv:2302.10207.
- Reindl, N. et al., 2023. The bright blue side of the night sky: Spectroscopic survey of bright and hot (pre-) white dwarfs. *A&A* 677, A29. doi:10.1051/0004-6361/202346865, arXiv:2307.03721.
- Ren, J. J. et al., 2020. The White Dwarf Binary Pathways Survey. V. The Gaia White Dwarf Plus AFGK Binary Sample and the Identification of 23 Close Binaries. *ApJ* 905, 38. doi:10.3847/1538-4357/abc017, arXiv:2010.02885.
- Ren, L., Li, C., Ma, B., Cheng, S., Huang, S.J., Tang, B., Hu, Y.m., 2023. A Systematic Search for Short-period Close White Dwarf Binary Candidates Based on Gaia EDR3 Catalog and Zwicky Transient Facility Data. *ApJS* 264, 39. doi:10.3847/1538-4365/aca09e, arXiv:2302.02802.
- Renedo, I., Althaus, L.G., Miller Bertolami, M.M., Romero, A.D., Córscico, A.H., Rohrmann, R.D., García-Berro, E., 2010. New Cooling Sequences for Old White Dwarfs. *ApJ* 717, 183–195. doi:10.1088/0004-637X/717/1/183, arXiv:1005.2170.
- Richer, H. B. et al., 2021. Massive White Dwarfs in Young Star Clusters. *ApJ* 912, 165. doi:10.3847/1538-4357/abdeb7, arXiv:2101.08300.
- Richer, H. B. et al., 2013. Comparing the White Dwarf Cooling Sequences in 47 Tuc and NGC 6397. *ApJ* 778, 104. doi:10.1088/0004-637X/778/2/104, arXiv:1310.0111.

- Rix, H.-W. et al., 2021. Selection Functions in Astronomical Data Modeling, with the Space Density of White Dwarfs as a Worked Example. *AJ* 162, 142. doi:10.3847/1538-3881/ac0c13, arXiv:2106.07653.
- Rogers, L. K. et al., 2024a. Seven white dwarfs with circumstellar gas discs I: white dwarf parameters and accreted planetary abundances. *MNRAS* 527, 6038–6054. doi:10.1093/mnras/stad3557, arXiv:2311.14048.
- Rogers, L. K. et al., 2024b. WD 0141-675: a case study on how to follow-up astrometric planet candidates around white dwarfs. *MNRAS* 527, 977–990. doi:10.1093/mnras/stad3098, arXiv:2310.05778.
- Rolland, B., Bergeron, P., Fontaine, G., 2018. On the Spectral Evolution of Helium-atmosphere White Dwarfs Showing Traces of Hydrogen. *ApJ* 857, 56. doi:10.3847/1538-4357/aab713, arXiv:1803.05965.
- Rolland, B., Bergeron, P., Fontaine, G., 2020. A Convective Dredge-up Model as the Origin of Hydrogen in DBA White Dwarfs. *ApJ* 889, 87. doi:10.3847/1538-4357/ab6602, arXiv:2001.01085.
- Romero, A. D. et al., 2022. Discovery of 74 new bright ZZ Ceti stars in the first three years of TESS. *MNRAS* 511, 1574–1590. doi:10.1093/mnras/stac093, arXiv:2201.04158.
- Romero, A.D., Kepler, S.O., Joyce, S.R.G., Lauffer, G.R., Córscico, A.H., 2019. The white dwarf mass-radius relation and its dependence on the hydrogen envelope. *MNRAS* 484, 2711–2724. doi:10.1093/mnras/stz160, arXiv:1901.04644.
- Rowell, N., Kilic, M., 2019. The kinematics of Galactic disc white dwarfs in Gaia DR2. *MNRAS* 484, 3544–3551. doi:10.1093/mnras/stz184, arXiv:1901.04948.
- Sahu, S. et al., 2023. An HST COS ultraviolet spectroscopic survey of 311 DA white dwarfs - I. Fundamental parameters and comparative studies. *MNRAS* 526, 5800–5823. doi:10.1093/mnras/stad2663, arXiv:2309.00239.
- Sahu, S. et al., 2022. Globular Cluster UVIT Legacy Survey (GlobULeS) - I. FUV-optical colour-magnitude diagrams for eight globular clusters. *MNRAS* 514, 1122–1139. doi:10.1093/mnras/stac1209, arXiv:2204.12886.

- Salaris, M., Bedin, L.R., 2018. A Gaia DR2 view of white dwarfs in the Hyades. *MNRAS* 480, 3170–3176. doi:10.1093/mnras/sty2096, arXiv:1809.09198.
- Salaris, M., Bedin, L.R., 2019. Praesepe white dwarfs in Gaia DR2. *MNRAS* 483, 3098–3107. doi:10.1093/mnras/sty3316, arXiv:1811.12825.
- Salaris, M., Cassisi, S., Pietrinferni, A., Hidalgo, S., 2022. The updated BASTI stellar evolution models and isochrones - III. White dwarfs. *MNRAS* 509, 5197–5208. doi:10.1093/mnras/stab3359, arXiv:2111.09285.
- Sanderson, H., Bonsor, A., Mustill, A., 2022. Can Gaia find planets around white dwarfs? *MNRAS* 517, 5835–5852. doi:10.1093/mnras/stac2867, arXiv:2206.02505.
- Saumon, D., Blouin, S., Tremblay, P.E., 2022. Current challenges in the physics of white dwarf stars. *Physics Reports* 988, 1–63. doi:10.1016/j.physrep.2022.09.001, arXiv:2209.02846.
- Shahaf, S., Bashi, D., Mazeh, T., Faigler, S., Arenou, F., El-Badry, K., Rix, H.W., 2023. Triage of the Gaia DR3 astrometric orbits - I. A sample of binaries with probable compact companions. *MNRAS* 518, 2991–3003. doi:10.1093/mnras/stac3290, arXiv:2209.00828.
- Shahaf, S., Hallakoun, N., Mazeh, T., Ben-Ami, S., Rekhi, P., El-Badry, K., Toonen, S., 2024. Triage of the Gaia DR3 astrometric orbits. II. A census of white dwarfs. *MNRAS* 529, 3729–3743. doi:10.1093/mnras/stae773, arXiv:2309.15143.
- Shariat, C., Naoz, S., Hansen, B.M.S., Angelo, I., Michaely, E., Stephan, A.P., 2023. Dynamical Evolution of White Dwarfs in Triples in the Era of Gaia. *ApJL* 955, L14. doi:10.3847/2041-8213/acf76b, arXiv:2306.13130.
- Shen, K.J., Blouin, S., Breivik, K., 2023. The Q Branch Cooling Anomaly Can Be Explained by Mergers of White Dwarfs and Subgiant Stars. *ApJL* 955, L33. doi:10.3847/2041-8213/acf57b, arXiv:2308.04559.
- Shen, K. J. et al., 2018. Three Hypervelocity White Dwarfs in Gaia DR2: Evidence for Dynamically Driven Double-degenerate Double-detonation

- Type Ia Supernovae. *ApJ* 865, 15. doi:10.3847/1538-4357/aad55b, arXiv:1804.11163.
- Steen, M., Hermes, J.J., Guidry, J.A., Paiva, A., Farihi, J., Heintz, T.M., Ewing, B.B., Berry, N., 2024. Measuring White Dwarf Variability from Sparsely Sampled Gaia DR3 Multi-Epoch Photometry. arXiv e-prints , arXiv:2404.02201doi:10.48550/arXiv.2404.02201, arXiv:2404.02201.
- Subasavage, J. P. et al., 2017. The Solar Neighborhood. XXXIX. Parallax Results from the CTIOPI and NOFS Programs: 50 New Members of the 25 parsec White Dwarf Sample. *AJ* 154, 32. doi:10.3847/1538-3881/aa76e0, arXiv:1706.00709.
- Swan, A., Farihi, J., Koester, D., Hollands, M., Parsons, S., Cauley, P.W., Redfield, S., Gänsicke, B.T., 2019. Interpretation and diversity of exoplanetary material orbiting white dwarfs. *MNRAS* 490, 202–218. doi:10.1093/mnras/stz2337, arXiv:1908.08047.
- Swan, A., Farihi, J., Melis, C., Dufour, P., Desch, S.J., Koester, D., Guo, J., 2023. Planetesimals at DZ stars - I. Chondritic compositions and a massive accretion event. *MNRAS* 526, 3815–3831. doi:10.1093/mnras/stad2867, arXiv:2309.06467.
- Temmink, K.D., Toonen, S., Zapartas, E., Justham, S., Gänsicke, B.T., 2020. Looks can be deceiving. Underestimating the age of single white dwarfs due to binary mergers. *A&A* 636, A31. doi:10.1051/0004-6361/201936889, arXiv:1910.05335.
- Toonen, S., Hollands, M., Gänsicke, B.T., Boekholt, T., 2017. The binarity of the local white dwarf population. *A&A* 602, A16. doi:10.1051/0004-6361/201629978, arXiv:1703.06893.
- Toonen, S., Nelemans, G., Portegies Zwart, S., 2012. Supernova Type Ia progenitors from merging double white dwarfs. Using a new population synthesis model. *A&A* 546, A70. doi:10.1051/0004-6361/201218966, arXiv:1208.6446.
- Torres, S., Canals, P., Jiménez-Esteban, F.M., Rebassa-Mansergas, A., Solano, E., 2022. A population synthesis fitting of the Gaia resolved white dwarf binary population within 100 pc. *MNRAS* 511, 5462–5474. doi:10.1093/mnras/stac374, arXiv:2202.04199.

- Torres, S., Cantero, C., Rebassa-Mansergas, A., Skorobogatov, G., Jiménez-Esteban, F.M., Solano, E., 2019. Random Forest identification of the thin disc, thick disc, and halo Gaia-DR2 white dwarf population. *MNRAS* 485, 5573–5589. doi:10.1093/mnras/stz814, arXiv:1903.07362.
- Torres, S. et al., 2023. White dwarf spectral type-temperature distribution from Gaia DR3 and the Virtual Observatory. *A&A* 677, A159. doi:10.1051/0004-6361/202346977, arXiv:2307.13629.
- Torres, S., Rebassa-Mansergas, A., Camisassa, M.E., Raddi, R., 2021. The Gaia DR2 halo white dwarf population: the luminosity function, mass distribution, and its star formation history. *MNRAS* 502, 1753–1767. doi:10.1093/mnras/stab079, arXiv:2101.03341.
- Tout, C.A., Wickramasinghe, D.T., Liebert, J., Ferrario, L., Pringle, J.E., 2008. Binary star origin of high field magnetic white dwarfs. *MNRAS* 387, 897–901. doi:10.1111/j.1365-2966.2008.13291.x, arXiv:0805.0115.
- Tremblay, P.E., Cukanovaite, E., Gentile Fusillo, N.P., Cunningham, T., Hollands, M.A., 2019a. Fundamental parameter accuracy of DA and DB white dwarfs in Gaia Data Release 2. *MNRAS* 482, 5222–5232. doi:10.1093/mnras/sty3067, arXiv:1811.03084.
- Tremblay, P.-E. et al., 2019b. Core crystallization and pile-up in the cooling sequence of evolving white dwarfs. *Nature* 565, 202–205. doi:10.1038/s41586-018-0791-x, arXiv:1908.00370.
- Tremblay, P. E. et al., 2017. The Gaia DR1 mass-radius relation for white dwarfs. *MNRAS* 465, 2849–2861. doi:10.1093/mnras/stw2854, arXiv:1611.00629.
- Tremblay, P. E. et al., 2020. Gaia white dwarfs within 40 pc - I. Spectroscopic observations of new candidates. *MNRAS* 497, 130–145. doi:10.1093/mnras/staa1892, arXiv:2006.00965.
- Tremblay, P.E., Leggett, S.K., Lodieu, N., Freytag, B., Bergeron, P., Kalirai, J.S., Ludwig, H.G., 2014. White Dwarfs in the UKIRT Infrared Deep Sky Survey Data Release 9. *ApJ* 788, 103. doi:10.1088/0004-637X/788/2/103.

- Tremblay, P.E., Ludwig, H.G., Steffen, M., Freytag, B., 2013. Spectroscopic analysis of DA white dwarfs with 3D model atmospheres. *A&A* 559, A104. doi:10.1051/0004-6361/201322318, arXiv:1309.0886.
- van Horn, H.M., 1968. Crystallization of White Dwarfs. *ApJ* 151, 227. doi:10.1086/149432.
- van Roestel, J. et al., 2021. A Systematic Search for Outbursting AM CVn Systems with the Zwicky Transient Facility. *AJ* 162, 113. doi:10.3847/1538-3881/ac0622, arXiv:2105.02261.
- van Roestel, J. et al., 2022. Discovery and characterization of five new eclipsing AM CVn systems. *MNRAS* 512, 5440–5461. doi:10.1093/mnras/stab2421, arXiv:2107.07573.
- Vanderburg, A. et al., 2020. A giant planet candidate transiting a white dwarf. *Nature* 585, 363–367. doi:10.1038/s41586-020-2713-y, arXiv:2009.07282.
- Vauclair, G., Schmidt, H., Koester, D., Allard, N., 1997. White dwarfs observed by the HIPPARCOS satellite. *A&A* 325, 1055–1062.
- Venner, A., Blouin, S., Bédard, A., Vanderburg, A., 2023. A crystallizing white dwarf in a sirius-like quadruple system. *MNRAS* 523, 4624–4642. doi:10.1093/mnras/stad1719, arXiv:2306.03140.
- Vennes, S., Kawka, A., Klein, B.L., Zuckerman, B., Weinberger, A.J., Melis, C., 2024. A cool, magnetic white dwarf accreting planetary debris. *MNRAS* 527, 3122–3138. doi:10.1093/mnras/stad3370, arXiv:2311.07937.
- Veras, D., 2021. Planetary systems around white dwarfs. Oxford Research Encyclopedia of Planetary Science URL: <http://dx.doi.org/10.1093/acrefore/9780190647926.013.238>, doi:10.1093/acrefore/9780190647926.013.238.
- Vincent, O., Barstow, M.A., Jordan, S., Mander, C., Bergeron, P., Dufour, P., 2024. Classification and parameterization of a large Gaia sample of white dwarfs using XP spectra. *A&A* 682, A5. doi:10.1051/0004-6361/202347694, arXiv:2308.05572.

- Vincent, O., Bergeron, P., Lafrenière, D., 2020. Searching for ZZ Ceti White Dwarfs in the Gaia Survey. *AJ* 160, 252. doi:10.3847/1538-3881/abbe20, arXiv:2010.02376.
- Wall, R.E., Kilic, M., Bergeron, P., Rolland, B., Genest-Beaulieu, C., Gianninas, A., 2019. GALEX absolute calibration and extinction coefficients based on white dwarfs. *MNRAS* 489, 5046–5052. doi:10.1093/mnras/stz2506, arXiv:1909.02617.
- Walters, N. et al., 2021. A test of the planet-star unipolar inductor for magnetic white dwarfs. *MNRAS* 503, 3743–3758. doi:10.1093/mnras/stab617, arXiv:2103.01993.
- Werner, K., Rauch, T., Kepler, S.O., 2014. New hydrogen-deficient (pre-) white dwarfs in the Sloan Digital Sky Survey Data Release 10. *A&A* 564, A53. doi:10.1051/0004-6361/201423441.
- Werner, K., Reindl, N., Rauch, T., El-Badry, K., Bédard, A., 2024. The photospheres of the hottest fastest stars in the Galaxy. *A&A* 682, A42. doi:10.1051/0004-6361/202348286, arXiv:2311.13388.
- Xu, S., Lai, S., Dennihy, E., 2020. Infrared Excesses around Bright White Dwarfs from Gaia and unWISE. I. *ApJ* 902, 127. doi:10.3847/1538-4357/abb3fc, arXiv:2009.00193.
- Xu, S., Rogers, L.K., Blouin, S., 2024. The chemistry of extra-solar materials from white dwarf planetary systems. arXiv e-prints , arXiv:2404.15425doi:10.48550/arXiv.2404.15425, arXiv:2404.15425.
- Yamaguchi, N., El-Badry, K., Rees, N., Shahaf, S., Mazeh, T., Andrae, R., 2024. Wide post-common envelope binaries from Gaia: orbit validation and formation models. arXiv e-prints , arXiv:2405.06020doi:10.48550/arXiv.2405.06020, arXiv:2405.06020.
- York, D. G. et al., 2000. The Sloan Digital Sky Survey: Technical Summary. *AJ* 120, 1579–1587. doi:10.1086/301513, arXiv:astro-ph/0006396.
- Zhang, H., Brandt, T.D., Kiman, R., Venner, A., An, Q., Chen, M., Li, Y., 2023. Dynamical masses and ages of Sirius-like systems. *MNRAS* 524, 695–715. doi:10.1093/mnras/stad1849, arXiv:2303.08198.

- Zubiaur, A., Raddi, R., Torres, S., 2024. A kinematic origin of the white dwarfs in the Solar neighborhood. arXiv e-prints , arXiv:2405.10380doi:10.48550/arXiv.2405.10380, arXiv:2405.10380.
- Zuckerman, B., Koester, D., Melis, C., Hansen, B.M., Jura, M., 2007. The Chemical Composition of an Extrasolar Minor Planet. ApJ 671, 872–877. doi:10.1086/522223, arXiv:0708.0198.